Faculty of Mathematical, Physical and Natural Sciences

Department of Materials Science

PhD in Nanostructures and Nanotechnologies

Development of a novel *Plasmodium falciparum* Topoisomerase I specific biosensor for diagnosis of malaria

Candidate: Cinzia Tesauro

Cycle: XXIII: 2007/2010

Supervisor: Prof. Alessandro Desideri

To
my parents,
my love and all my friends

INDEX

INTRODUCTION

Single molecule techniques to study the DNA-modifying enzymes

Nowadays molecular and cellular biologists are moving toward nano-techniques to perform experiments on single molecules rather than on populations of molecules (Koster *et al*, 2010; Subramani *et al*, 2010). Single-molecule techniques impacted biology (Sako and Yanagida, 2003) optics (Askhin, 1997; Kasparian and Wolf, 2008) and electronics (Cavallini *et al*, 2008; Kubatkin *et al*, 2003). In biological sciences, single-molecule detection has been a goal since the beginning of the era of molecular biology because these methods have a significant advantage: they can contrast with measurements on an ensemble or bulk collection of molecules where the individual behavior can not be distinguished and only average characteristics can be measured. Single-molecule experiments provide information on distributions and time trajectories for the study of proteins and other complex biological machinery that was limited using ensemble experiments that hardly make possible the direct observation of their kinetics. One of the most powerful examples is the single molecule fluorescence microscopy that enabled to understand the walking mechanisms of kinesin-myosin in muscles (Mikhailenko *et al*, 2010).
These technologies offer a broad spectrum of clinical and research applications: often is not enough to know whether a molecule is present but also the position of the molecule in the cell or tissue at the

time of detection may be important. One example can be on the human diagnostic, particularly regarding the cancer.

The development of single molecule detection techniques has opened new horizons for the study of individual macromolecules under physiological conditions. Recently it became possible to study the action of a single nucleic acid-modifying enzyme (polymerases, restriction enzymes, DNA topoisomerases, helicases) on a single DNA or RNA molecule in real time, obtaining information on the interaction between them with high detail (Yao *et al*, 2009). It's increasingly interesting to study the mechanical properties of DNA under torsional and tensional stress, and figure out which are the consequences of these stresses on the activity of DNA-modifying proteins (Neuman, 2010). Addressing these questions is essential to understand DNA dynamics and energetics within the cell and to discerne how the myriad of proteins that bind to and modify DNA are influenced by these properties.

Local force measurement techniques, such as atomic force microscopy (Nguyen *et al*, 2010), magnetic tweezers (Leuba *et al*, 2009) and optical trapping (Pope *et al,* 2002) have been used to study the elastic property of nucleic acids in combination with the structural transitions mediated by different enzymes.

AFM is a scanning probe microscopy technique that has been around for 2 decades. Because the atomic force microscope relies on the forces between a tip and a sample, knowing these forces is important for proper imaging. The force is not measured directly, but calculated by measuring the deflection of the lever, and knowing the stiffness of the cantilever. The AFM head uses an optical detection system in

which the tip is attached to a reflective cantilever. A diode laser is focused onto the back of a reflective cantilever; when the tip scans the sample surface, the laser beam is deflected from the position in the detector and the signal is the difference in light intensities (Engel and Muller, 2000). Although AFM has typically been used for topographical imaging applications, it has found applications in manipulating samples of all kinds, including in biological studies to look at the folding and unfolding of molecules (Wang K. *et al*, 2001).

In the field of DNA and DNA-enzyme interaction research, AFM has been involved in the study of chemical reactions at single molecule level. For example, these reactions can be performed and imaged at a local position on a DNA origami scaffold (Voigt *et al*, 2010). DNA origami is the nanoscale folding of DNA to create arbitrary two and three dimensional shapes at the nanoscale and recently a DNA origami platform has been used to monitor the interactions between a single human topoisomerase I covalently bound to one DNA fragment and a second DNA fragment protruding from the DNA origami itself (Subramani *et al*, 2010).

There are different approaches to decipher protein-DNA interactions but the most powerful consists in the direct observation of proteins bound to DNA under well-controlled conditions.

DNA-protein interactions can be detected, for example, using an unzipping apparatus (in which the dsDNA is mechanically forced to be opened), because the binding of an enzyme to dsDNA transiently blocks the opening fork. Another class of experiments uses the differences between the elasticieties of ssDNA and dsDNA, or the dependence of dsDNA elasticity on twist. From this point of view,

pulling a single molecule of DNA from its opposite ends permit to observe the enzymatic activity that transform, for example, the torsional state of dsDNA without enzyme immobilization, i.e in solution (Strick *et al*, 2000; Koster *et al*, 2005) (FIG 1).

A typical magnetic tweezers instrument consists of a pair of small permanent magnets, arranged with their opposite poles separated by a small gap, placed above a flow cell on an inverted microscope.

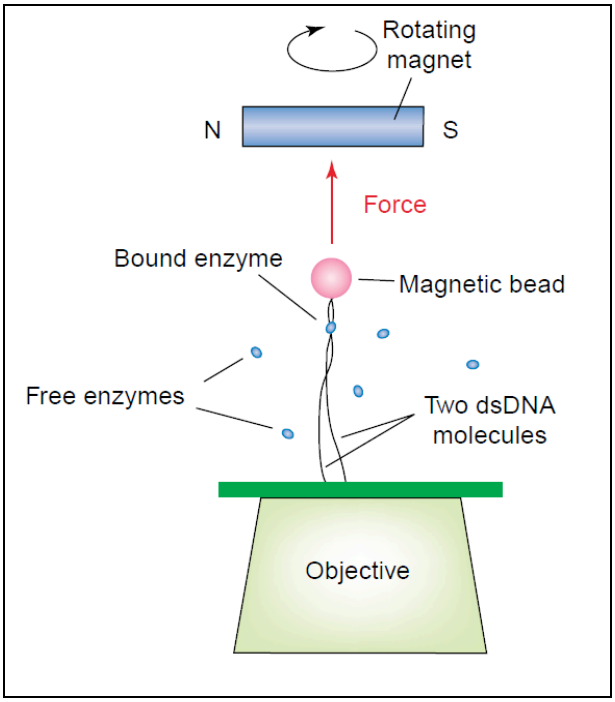

Figure 1. Setup for single molecule analysis of DNA interacting enzyme: DNA unlinking by topoisomerase (Bockelmann, 2004).

DNA is attached to the anti-digoxigenin-coated surface of the flow cell via multiple digoxigenin moieties incorporated in one end of the

DNA. The free end of the DNA is attached to a streptavidin-coated superparamagnetic bead via multiple biotin moieties. The magnets above the flow cell impose an upward force on the magnetic bead that can be controlled by changing the vertical position of the magnets. The magnetic moment of the bead is entrained by the field of the external magnets so that it rotates in a one-to-one correspondence with magnet rotation. An high-magnification objective images the bead onto a charged-couple device camera, and the three-dimensional position of the bead is obtained in real time. With this relatively simple setup, linking number (explained later) of individual DNA molecules, subjected to well controlled pulling forces, can be precisely controlled and the corresponding changes in DNA extension can be measured with high accuracy.

Optical tweezers instead allow the accurate study of DNA dynamics. In the context of DNA supercoiling, they have been used to unzip DNA (van Mameren *et al*, 2008). Optical tweezers are true ‘‘tweezers’’: beads can be picked up and moved around by means of a laser beam. One can suspend individual biomolecules, such as DNA between two beads, and stretch the molecule by moving the beads away from each other (Neuman and Block, 2004).

For instance, in the double-trap transcription experiment used to investigate the proof reading mechanism of RNA polymerase (Shaevitz *et al*, 2003), a stalled complex, consisting of a biotin-tagged RNA polymerase and a digoxigenin-terminated DNA template, is attached between two polystyrene beads of different size. Each of the two beads is held in a separate optical trap. The tension in the molecular construct is kept nearly constant by feedback control of the

position of the optical trap holding the larger bead. Transcription is recorded by monitoring the position of the smaller bead (FIG 2).

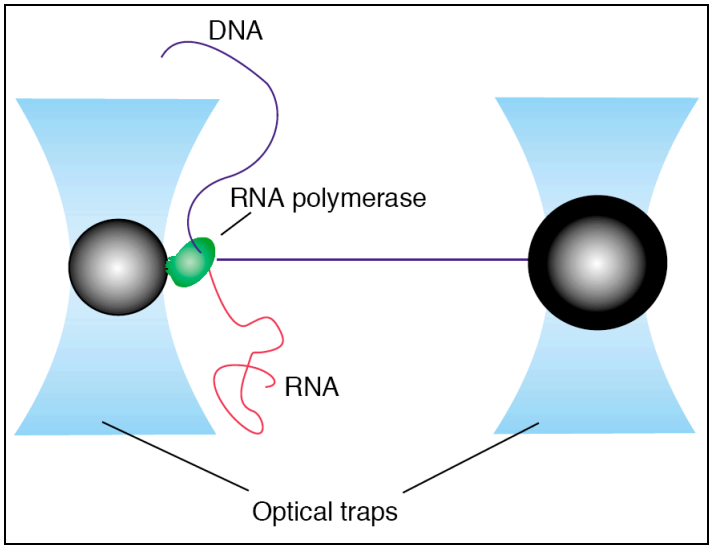

Figure 2. Optical tweezers setup to study the RNA polymerase mechanism (Bockelman, 2004).

In all the above explained experiments short DNA fragments are used, free in solution or commonly attached to a surface but in the organism DNA molecules are very long and flexible. These assays are used to study the action of protein interacting with DNA but indirectly by measuring changes in the physical properties of the DNA strands. Such methods have proven to be very powerful, requiring only trace amount of protein but they have limited capacities of multiplexing (detection of numerous target at the same time).

From a practical point of view, these techniques involve multiple time consuming steps, expensive equipment and well-trained and competent scientist that make them hardly adaptable to other

purposes. These aspects are not despensable for the advancement of single-molecule assays toward applications in diagnostic, genomic analysis and drug screening.

Rolling circle amplification

Tecniques for single molecule detection must be highly sensitive; the possibility to detect without the need of a complex instrumentation has increased in the recent years so novel assays are being developed for detection of nucleotide sequences or protein activities at the nanoscale or single molecule level (Hammond, 2006; Seidel and Dekker, 2007). The field of DNA diagnostic has been revolutionized by the advent of powerful nucleic acid amplification technologies such as the polymerase chain reaction, PCR (Winn-Deen, 1996). Numerous clinical diagnostic tests, now in use or under development, are based on the extreme sensitivity of these amplification methods. Such tests have reduced the time required for detection, for example of infectious agents, from weeks or days to hours and allow for detection of DNA traces in forensic samples where was not previously possible. New tests are being developed to detect rare mutations in patient's samples to diagnose genetic diseases or cancer at the earliest possible stage.

Since sequence data of the entire human genome became available, there is a continuing need for rapid and sensitive tests to analyze polymorphisms in individual samples at the single nucleotide level. In 1990 it was discovered that certain polymerase enzymes are able to

effectively perform nucleic acid synthesis, then termed rolling-circle replication, using a single stranded DNA (ssDNA) minicircle as a template (Fire and Xu, 1995). It's a process of unidirectional nucleic acid synthesis that can lead to the formation of multiple copies of circular DNA or RNA, such as plasmids, the genomes of bacteriophages and the circular RNA genome of viroids (FIG 3) (Johne *et al*, 2009).

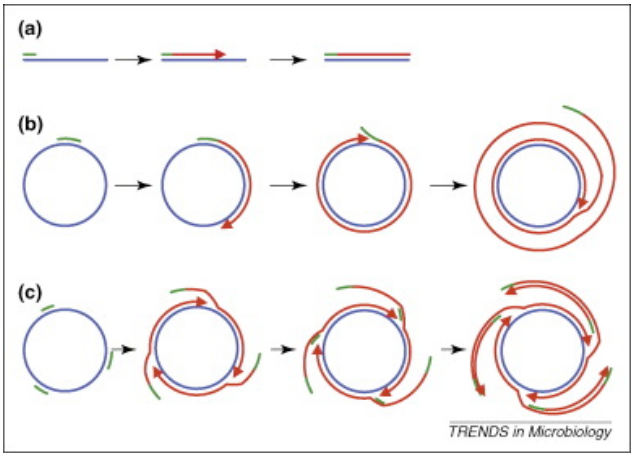

Figure 3. Principle of rolling-circle replication. Blue lines denote target DNA sequences, green lines represent oligonucleotide primers and red lines represent new DNA synthesized by the polymerase. Arrow heads indicate 3′ ends of growing DNA strands. (a) Linear template and single primer. After primer binding, the polymerase synthesizes one complementary strand. (b) Circular template and single primer. The polymerase synthesizes a complementary strand beginning at the bound primer. After one round, the primer and the synthesized strand are displaced and DNA synthesis continues for additional rounds. By this, a long concatemeric single-stranded DNA is produced. (c) Circular template and multiple random primers. The synthesis is initiated at multiple primers bound to the template. DNA synthesis using strand displacement is carried out as in (b). However, primers still present in the reaction mixture bind to the displaced strand and are used as additional initiation points for DNA synthesis. The multiple products are long concatemeric molecules of double-stranded DNA (Johne *et al*, 2009).

In case of a linear template molecule and a single primer, after the primer binding the polymerase synthesizes one complementary strand (FIG 3a), and the synthesis is completed at the end of the template.

For a circular template molecule (FIG 3b), synthesis is presumed to begin at a specific initiation point on the template ring. One strand of the parental duplex ring is cut at a specific point by an endonuclease. This enzyme recognizes a particular sequence at this point. As result of the cut ('nick'), a linear strand with 3' and 5' ends is created.

The 3' end serves as a primer for the synthesis of a new DNA strand under the catalytic action of DNA polymerase. The unbroken strand is used as the template for this purpose, and a complementary strand is synthesized. In this way, the parental molecule itself is used as a primer for initiating replication. The polymerase displaces the newly synthesized strand and goes on with DNA synthesis for several rounds, dependent on the template length. By this mechanism, a large DNA molecule consisting of repeated copies of the template sequence is produced, leading to a more efficient amplification of a circular target sequence as compared to a linear template (Gilbert and Dressler, 1968).

By adding an additional primer with a binding site on the complementary strand, a more efficient amplification is observed for both kinds of templates as this primer can bind to the displaced strand and initiate additional DNA synthesis. In this case, the amplification products consist of double-stranded DNA (FIG 3c).

This kind of replication has gained much interest because it has been adapted to be used in one of the most promising single molecule detection system, the so called rolling circle amplification (RCA).

There are other several isothermal methods of probe, signal and target DNA amplification such as branched probes (Shchepinow *et al*, 1997), strand displacement approach (Walker *et al*, PNAS 1992; Walker *et al*, 1992) and others, but all of them are rather complicate and require an assay optimization. RCA based assays don't require preoptimization of the experimental set up and protocol. Moreover RCA approaches have been attracting attention of diagnostic-oriented biotech companies because of their simplicity, high sensitivity, large multiplex potential, compatibility with other detection/imaging techniques and immunity to false positive and cross contamination (that could happen in the most widely used laboratory technique, PCR). RCA has become the most important isothermal DNA amplification method used in basic and applied research (Lizardi *et al*, 1998).

RCA driven by DNA polymerase can replicate circularized oligonucleotide probes without the use of complex and expensive devices. These circularized oligonucleotides templates, called "padlock probes" were first reported by Nilsson in 1994 (Nilsson *et al*, 1994). Padlock probes are synthetic single stranded DNA molecule that can be circularized by enzymatic ligation upon annealing to a specific target or as result of a specific protein recognition reaction using a modified version of the proximity ligation. These "padlock" probes are composed of two target complementary sequences located at the 5´and 3´termini (FIG 4, black segments), connected by a linker that may carry detectable functions (FIG 4, grey segment). The two ends of the linear oligonucleotide probe are brought in juxtaposition by hybridization to a target sequence. This juxtaposition allows the

two probe segments to be covalently joined by the action of a DNA ligase that requires a dsDNA to act. Following ligation the probe is wrapped around the target sequence, thereby topologically locking the probe to the target and then the circle can be amplified by rolling circle DNA synthesis and detected.

Padlock probes offer great specificity and less background and have the adantage in terms of detection sensitivity compared to conventional oligonucleotide probes (Liu *et al*, 1996).

The nature of these circularized probes imparts diverse applications in clinic, research and drug discovery including in situ detection, microarrays, immunoassays and single nucleotid polymorphism (SNP) detection (Bàner *et al*, 1998). The ligation event, infact, allows for discrimination of minor variations in sequence so padlock probes have been optimized for the SNP detection (FIG 4).

Nilsson and Koch were able to distinguish between single nucleotide variants also on centromeric DNA in methaphase preparation (Nilsson *et al*, 1997) demonstrating that padlock probes offer the possibility of higly sensitive detection *in situ.*

Following the RCA each circularized probe is transformed in to a rolling circle product (RCP) that consist in a multiple (up to 10^3) tandem copies of the padlock probes. The RCPs can be hybridized with fluorescent probes and optically detected at the microscope or using microfluidic analysis (Jarvius *et al*, 2006). In this way, RCPs become adaptable for the multiplexed detection of several target at the same time, being hybridizable with different labeled probes.

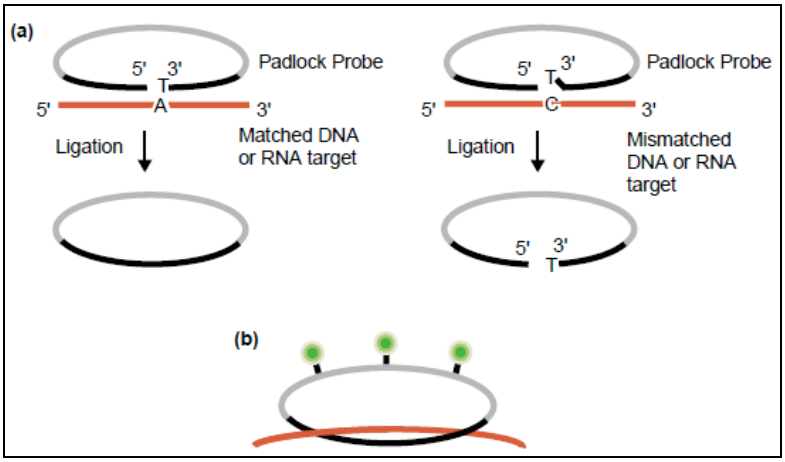

Figure 4. Schematic representation of padlock probes and means to detect reacted probes. **(a)** Padlock probe (black and gray) hybridization to a target DNA or RNA sequence (red). The padlock probe can be converted to a circle by a ligase (left), but ligation is inhibited if the ends of the probe are mismatched to their target and the probe remains linear (right). **(b)** Direct detection of a reacted probe, catenated to a target sequence. Following washes and/or exonuclease treatment, a bound probe is visualized via detectable functions (green) attached to the linker segment (Bàner, 2001).

DNA topology and DNA topoisomerases

DNA length can be thousands of times greater of a cell dimension so its packaging within the nucleus is permitted by its supercoiling that reduce its volume. In prokaryotes DNA is in a plectonemic supercoiled state that permits the genome of these organisms to be organized into a small closed circular chromosome (Vologodskii and Cozzarelli, 1994). However, in eukaryots, DNA supercoiling occurs also in a solenoid structure, with the help of histones that are more effective for DNA compaction. An important topologic property of a DNA molecule is the linking number (Lk) that is merely the number of crosses a single strand makes across the other in a planar projection. Lk depends on two geometric properties, the twist (Tw) and the writhe (Wr). Tw is the number of twists or turns of the double helix, and Wr is the number of coils or 'writhes'. The topology of the DNA is then described by the equation: Lk = Tw + Wr; if there is a closed DNA molecule, the sum of Tw and Wr, or the linking number, does not change but there may be complementary changes in Tw and Wr without changing their sum. Changes in Lk are always integers and it's necessary to break at least one of the DNA strands to introduce changes in Lk.

The integrity and the physical organization of DNA must be manteined to ensure the survival of cells. Many essential cellular processes can cause problems in the topological structure of DNA. In particular, the separation of the two strands of the double helics generates tensions and other topological stresses that must be resolved

in order to complete DNA metabolism processes such as replication, transcription and recombination (Wang, 1996; Champoux, 2001). These problems can be solved by a class of ubiquitous enzymes that are called DNA topoisomerases, discovered by James C. Wang in 1971 (Wang, 1971).

DNA topoisomerases (Top) helps to solve topological problems by introducing single or double transient strand breaks followed by a religation of the scissile strands; in this way they change the linking number and the supercoiling state of DNA (FIG 5a). The reaction catalized by topoisomerases consist of a cleavage that occurs with an initial transesterification reaction between a tyrosine of the active site of the protein and a phosphate group of the DNA; this lead to the formation of a covalent intermediate enzyme-DNA complex. Then DNA is released through a second transesterification reaction (Wang, 2002).

There are topoisomerases that only relax negative supercoils, others relax both signs and some even introduces negative (such as bacterial DNA gyrase) or positive (reverse gyrase) supercoils. The classification of topoisomerases is based on the number of DNA strands cleaved during the catalytic reaction (FIG 5b).

Topoisomerases that cleaves only one strand are defined as type I, those that cleaves both strands, generating a cleaved staggered duplex filament, are classified as type II topoisomerases (Champoux, 2001). Type I topoisomerases are monomeric (with the exception of the heterodimeric enzyme described in Kinetoplastida) and are further classified into two subfamilies: IA and IB. The IA family introduces positive supercoils, decatenate single-stranded DNA and unwind

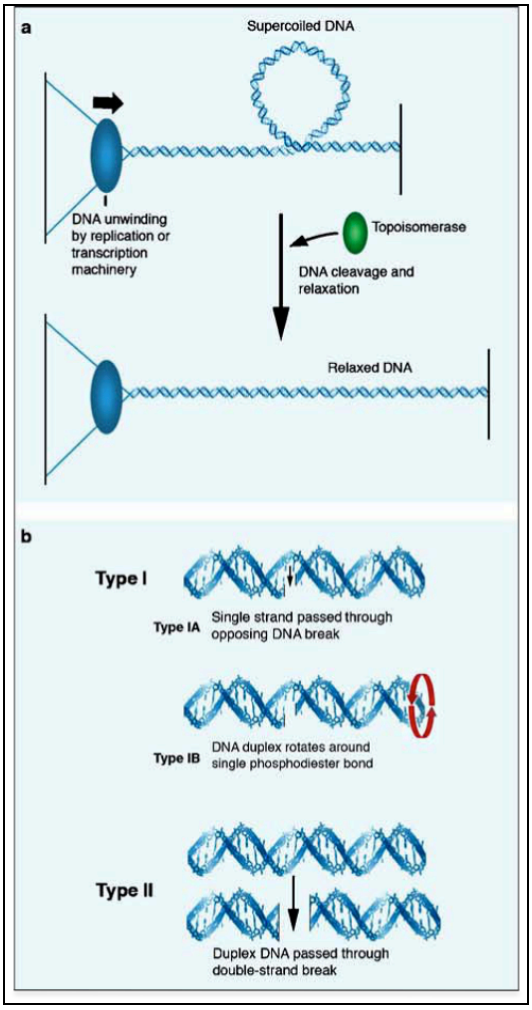

Figure 5. a) The double helices separation lead to the formation of supercoils that are relaxad by topoisomerase. b) Two classes of topoisomerases and their mechanism (Leppard, 2005).

supercoiled DNA through covalent binding to the the 5' end of the scissile strand, leaving a free 3'-OH strand. Top IB family relax both

negatively and positively supercoiled DNA, establishing temporary phosphotyrosine bonds with the 3' end and leaving a free 5'-OH strand. The type II topoisomerases are homodimers or heterodimers and form the covalent intermediate by binding at the 5' end (Corbett and Berger, 2004). All the topoisomerase world can now be described in the framework of these four families (Topo IA, Topo IB, Topo IIA, Topo IIB), with the exception of the stand-alone TopoV, a DNA topoisomerase discovered in 1992 which is only present in one species, the archaeon Methanopyrus kandleri (Slesarev, 1993).

DNA topoisomerase IB (TopIB)

Type IB topoisomerases fall into two highly related but separate structural categories. The first category includes the viral type TopIB, exemplified by vaccinia topoisomerase I (v-topo I). The second type TopIB category includes the eukaryotic enzymes, typified by the well-studied human topoisomerase I, hTopI (Leppard and Champoux, 2005). The ability to relax DNA supercoils allows these proteins to play an essential role during replication (Yang *et al*, 1987), transcription (Gilmour and Elgin, 1987), recombination (Bullock *et al*, 1985) and chromosome segregation (Maul *et al*, 1986); TopIB can relax the positive supercoils that accumulate ahead of the movement of polymerases, a task that is confined to TopII in bacteria. Relaxation occurs by "controlled rotation" mechanism (FIG 6) because the unbound 5´OH is free to rotate prior to religation (Stewart *et al*, 1998)

except for friction between the rotating DNA and the enzyme cavity (Koster *et al,* 2005).

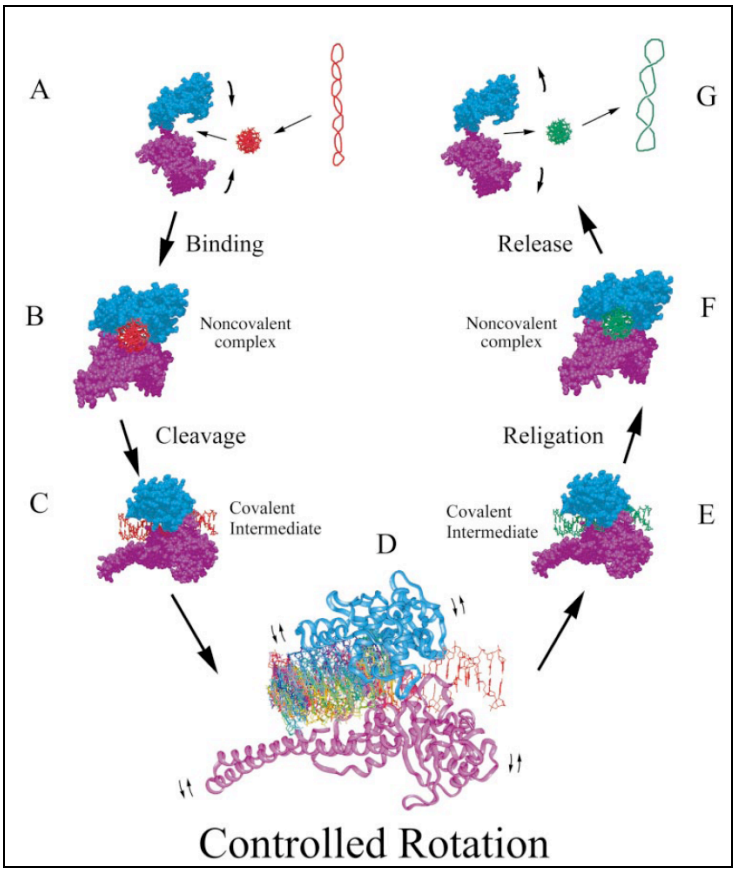

Figure 6. Controlled rotation mechanism of human topoisomerase IB, as an example for TopIB family (Stewart, 1998).

The catalytic cycle of TopIB consist of:

- Binding to DNA (FIG 6A)

- A trans-esterification reaction between the hydroxyl group of a tyrosine residue, placed at the active centre, which provides a transient covalent bond with the 3´end of the cleaved strand (FIG 6B-C)
- Relaxation of DNA that is propelled by the superhelical tension (FIG 6D)
- Resealing of the phosphodiester bond using the energy stored in the DNA-TopIB complex (FIG 6E-F)
- Releasing of DNA, restoring the integrity of the double helix (FIG 6G).

As the energy of the phosphodiester bond is conserved in the protein-DNA covalent intermediate, the cleavage-religation step does not require ATP hydrolysis. Unlike TopIA, DNA relaxation does not require Mg^{2+} and the polarity of covalent complex formation is different.

Topo IB are ubiquitous in eukaryotes, where they represent the major DNA topoisomerase I activity. Two different Topo IB are present in vertebrates, one localized in the nucleus and the other in the mitochondria (Zhang *et al*, 2004). Eukaryotic Topo IB are large monomeric enzymes (around 90 kDa) with a highly conserved DNA binding domain and a C-terminal catalytic domain, linked by a non conserved hydrophilic region. TopIB sequences are also found in all currently sequenced poxviruses genomes. Until recently, TopIB have been thought to be specific for eukaryotes and poxviruses. However, the discovery of TopIB in some bacteria recently broke this rule (Krogh and Shuman, 2002). As for TopIA, several structures of TopIB are now available, and cover the three different subfamilies, the viral vaccinia TopI (Sharma *et al*, 2004), the eukaryotic one (human TopIB;

Redinbo *et al*, 1998) and the recently discovered bacterial one (*Deinococcus radiodurans* TopIB; Patel *et al*, 2006).

The best studied of the cellular type IB enzymes is the human TopIB. Based on sequence comparisons, it is likely that most features described for the human enzyme are applicable to the cellular topoisomerases I from other eukaryotic species. As a type IB enzyme, topoisomerase I can relax positive and negative supercoils; it is responsible for relieving the torsional stress associated with DNA replication, transcription, and chromatin condensation (Champoux *et al*, 2001; Wang *et al*, 2002). Furthermore, topoisomerase I is the only molecular target for the camptothecin class of anticancer drugs, which are used in the treatment of many types of cancers including colorectal and ovarian cancer (Garcia-Carbonero and Supko, 2002).

Based on conservation of sequence, sensitivity to limited proteolysis, X-rays analysis and fragment complementation experiments (Stewart *et al*, 1997) the 91-kDa human TopIB protein has been subdivided in to four distinct domains (FIG 7):

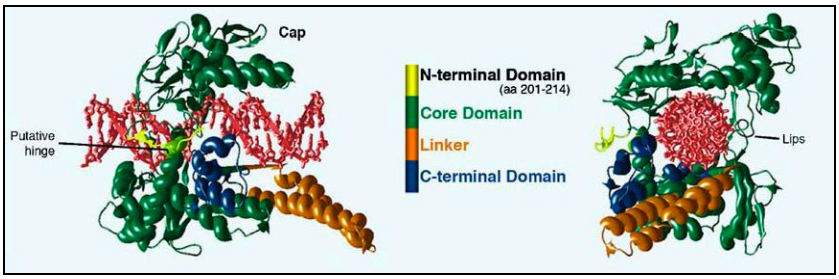

Figure 7. Domain organization of human TopIB (Leppard, 2005).

- An N-terminal domain (aa 1-214) that is poorly conserved, higly charged, protease sensitive, unstructured (it was not possible to crystallize it) and not required for activity in vitro, but does contain five nuclear localization signals presumably responsible for subcellular localization of the enzyme in vivo (Mo *et al*, 2000);
- An higly conserved Core domain (aa 215-635) that contains all the residues forming the active site (Arg488, Lys532, Arg590, His632) excluding the catalytic tyrosine (Tyr723). It is divided by convention into tree subdomains (FIG 7, green). Subdomains I and II form a 'cap' over bound DNA, contributing to a pair of α-helices, termed the 'nose cone'. The cap is connected to the core subdomain III by a short hinge helix, whereas core subdomain III and the C-terminal domain, which comprise the catalytic base of the enzyme, are split into two elements by the linker domain (Berger and Schoeffler, 2008);
- A protease sensitive and poorly conserved linker domain (aa 636-712) that is positively charged and organized into two long α-helices (α18 e α19) that form a 'coiled-coil' structure and protrudes from the base of the enzyme (FIG 7, orange). The linker helices are dispensable for relaxation activity but play a role in the DNA cleavage-religation equilibrium (Stewart *et al,* 1997). By crystallographic studies and by mutants analysis it is confirmed a role of this domain in the enzyme catalysis. In particular, it is observed that the mutation Ala653Pro increases the domain flexibility moving the cleavage-religation equilibrium toward the religation. This mutant shows also an high resistance to camptothecin (CPT) drug due to his fast religation that inhibits the entrance of CPT into the active site (Fiorani *et al.,* 2003);

- A conserved C- terminal domain (aa 713-765) that contains the catalytic Tyrosine (Tyr723) organized into five short α-helices (FIG 7, blue). The Tyr723 lodges on the loop connecting α-helices 20 to 21 and its mutation to phenylalanine inactivates the enzyme (Redinbo *et al*, 1998). The core and C-terminal domain form a clamp that encircles DNA in a positively charged central hole of 20 Å (FIG 6). The surface of this cavity host a lot of positive charged residues that interact with the negative charged surface of DNA.

The substrate specificity of eukaryotic topoisomerases I has been characterized at both the nucleotide sequence level and at the level of DNA tertiary structure. By mapping cleavage sites using detergent to trap the covalent complex (Tanizawa *et al*, 1993), the enzymes were found to nick the DNA with a preference for a combination of nucleotides that extends from positions -4 to -1 of the cleavage site.

The preferred nucleotides in the scissile strand are 5'-(A/T)(G/C)(A/T)T-3' with the enzyme covalently attached to the -1 T residue. Occasionally a C residue is found at the -1 position. A particularly strong cleavage site for all eukaryotic topoisomerases I was identified by Westergaard and his colleagues in the rDNA repeats found in *Tetrahymena pyriformis* and this sequence, which has a T at the -1 position, formed the basis for designing the 22 base pair oligonucleotide used in the crystallographic studies (Redinbo *et al*, 1998).

Clinical significance of Topoisomerases

DNA Topoisomerases are the targets of important anticancer and antibacterial drugs (Pommier *et al*, 2010). These enzymes are the molecular targets of a class of compound with anticancer effects so they play an important role in clinical terms. The research in this field has allowed to better understand the mechanism of action of Top and carried out the possibility to produce more effective and specific therapeutic drugs.

Inhibitors of TopI are divided into two classes: poisons and catalytic inhibitors (Holden, 2001). Poisons include clinically used drugs, such as the derivatives of the natural compound CPT (camptothecin) that reversibly bind the covalent TopI-DNA complex, slowing down the religation of the cleaved DNA strand thus inducing cell death. Infact trapped protein-DNA intermediates can lead to double strand breaks caused by collision with replication and transcription complexes (Rasheed and Rubin, 2003). Two water-soluble CPT derivatives, TPT (topotecan) and irinotecan, have been approved by the food and drug administration (FDA) for clinical use. Catalytic inhibitors act through inhibiting any other step of the TopI enzymatic cycle (Pommier, 2009; Tesauro *et al*, 2010). CPT act by stabilising the covalent DNA-enzyme intermediate that is converted to cytotoxic DNA lesions by collision with the replication (Hsiang *et al*, 1989) or transcription machinery (Wu and Liu, 1997). The cytotoxic effect of CPT is most prominent in the S-phase of the cell cycle, implying increased

sensitivity of rapidly dividing cells such as in cancer, bacterial infections and of course malaria.

In spite of the remarkable elucidation of topoisomerase structures, enzymatic mechanisms, biological functions, and mechanisms of action of inhibitors as antibacterial and anticancer agents over the past 30 years there are still no relevant inhibitors for viral, bacterial and protozoan type I topoisomerases.

The discovery of novel antibacterials (and antiprotozoan) not only against type II enzymes but also against type I topoisomerases is warranted. Such drugs could provide new therapies against human diseases, including bacterial or parasital infections associated with the emergence of highly resistant strains.

Biology of Malaria

Malaria is caused by infection of red blood cells with protozoan parasites of the genus Plasmodium. The parasites are inoculated into the human host by a feeding female mosquito of the Anopheles genus (FIG 8). The four Plasmodium species that infect humans are P. *falciparum*, P. *vivax*, P. *ovale* and P. *malariae*. There are about 380 species of anopheline mosquito, but only 60 or so are able to transmit the parasite. Like all other mosquitos, the anophelines breed in water, each species having its preferred breeding grounds, feeding patterns and resting place. Their sensitivity to insecticides is highly variable. Plasmodium parasite develops in the gut of the mosquito and is passed in the saliva of an infected insect each time it takes a new blood meal.

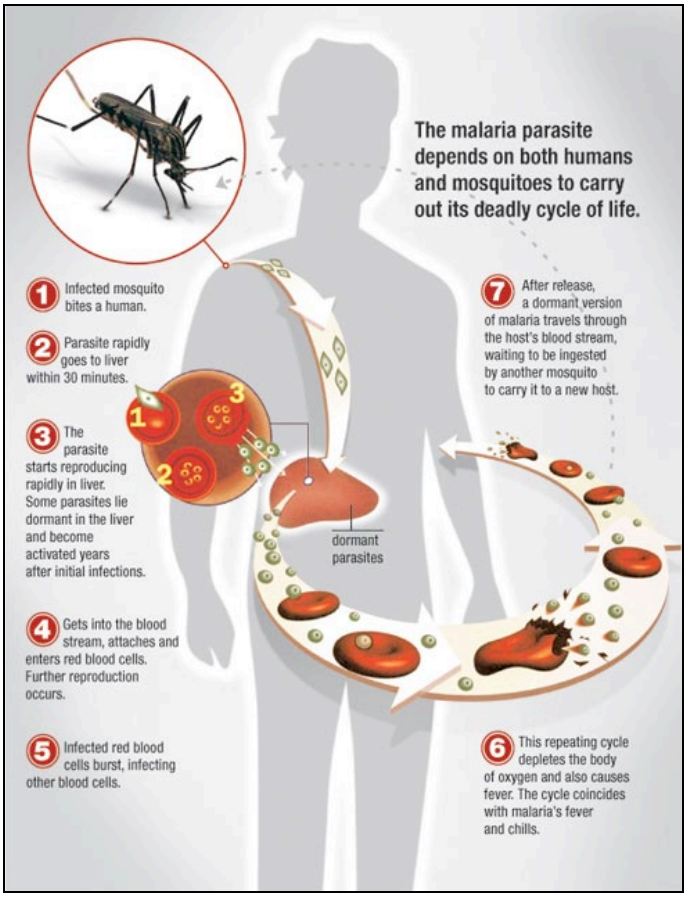

Figure 8. Lyfe Cycle of *Plasmodium falciparum.*

Within 30 minutes of being introduced into the human host, the sporozoites form of the parasite infected hepatocytes, multiplying asexually and asymptomatically for a period of 6-15 days (even if some parasites lie dormant in the liver and become activated years after initial infection).

Once in the liver, these organisms differentiate to yield thousands of merozoites, which, following rupture of their host cells, escape into the blood and infect red blood cells, thus beginning the erythrocytic stage of the life cycle (Miller *et al*, 2002). The parasite escapes from the liver undetected by wrapping itself in the cell membrane of the infected host liver cell (Sturm *et al*, 2006). Within the red blood cells, the parasites multiply further, again asexually, periodically breaking out of their hosts to invade fresh red blood cells.

Several such amplification cycles occur: each merozoite successfully invading a red blood cell (RBC) passes through three distinct stages of development: the relatively inert ring stage, a metabolically active trophozoite stage and the segmenting schizont stage. The parasite divides four times during schizogeny, yielding on average 16 new merozoites (Bannister *et al*, 2000) and thus an exponential amplification of the parasite population in the order of 16^n, with one intraerythrocytic cycle completed in 48hrs.

Malaria diagnostic tools

Malaria is an important cause of death and illness in children and adults, especially in tropical countries. The World Health Organization (WHO) estimates that half the world's population is at risk of malaria, with 243 million people developing clinical malaria (86% in Africa), with nearly 863,000 deaths (89% in Africa, most being children). Malaria remains endemic in 108 countries, and while parasite-based diagnosis is increasing, most suspected cases of malaria

are still not properly identified, resulting in over-use of anti-malarial drugs and poor disease monitoring (World Malaria Report, 2009). Malaria elimination has been achieved progressively in parts of the world since the recorded history of the disease. By the mid-19th century, malaria had been eliminated from several countries in temperate zones in which it had been endemic. In the context of the Global Malaria Eradication Programme (1955-1968) and up to 1987, 24 countries were certified as malaria-free. Since then, an additional 9 countries have reported (periods of) zero locally acquired cases, leading to a further contraction of the world map of malaria endemicity (Mendis *et al,* 2009)

Malaria is still today a disease of poverty in developing countries; in Africa mortality remains high because there is limited access to treatment in the villages. Once a person develops malaria, the only means of reducing suffering and preventing death is by diagnosing and treating the disease. The absolute necessity for rational therapy (considering also the increasing drug resistance) is based on the accuracy of malaria diagnosis.

For the last three quarters of last century, since the discovery and development of chloroquine in the 1930s and 40s, the medical community has treated most fevers in malaria-endemic countries as malaria, forgoing the diagnostic process. The common teaching has been "fever equals malaria unless proven otherwise" (Perkins and Bell, 2008). Malaria is frequently over-diagnosed on the basis of symptoms alone, especially in endemic areas, because of its non-specificity of symptomatology. At an early stage, with no evidence of vital organ dysfunction, the patients can readily be treated with full

rapid recovery provided prompt and effective treatment is given. If, however, ineffective medicines are given or if treatment is delayed, particularly in *P. falciparum* malaria, the parasite burden continues to increase and severe malaria may ensue. It's a progression that may occur within a few hours. Severe malaria usually manifests with one or more of the following: coma (cerebral malaria), metabolic acidosis, severe anaemia, hypoglycaemia, acute renal failure or acute pulmonary oedema. If left untreated, severe malaria is fatal in the majority of cases.

Clearly many lives have been saved by pushing for rapid, even community or home-based access to antimalarial. In the many communities in which malaria has accounted for the majority of potentially fatal causes of fever, it has been hard to imagine any other approach, given the poor performance and relative unavailability of microscopy. Over the past decade, though, a number of important changes have taken place in the epidemiology and control of malaria and in the diagnostic techniques available that dramatically alter the balance of rational action in favour of parasite-based diagnosis over blind therapy of fever with anti-malarial drugs. Specific diagnosis of malaria is now not only possible, but necessary, and scaled up malaria control efforts must include expanded and quality assured use of parasite based diagnostic testing.

Malaria diagnostic methods are divided in clinicals and biological.

Clinical diagnosis is less expensive and the most common used methods. However accuracy of clinical diagnosis varies with the level of endemicity, malaria season and age group; moreover the

overlapping of malaria symptoms with other tropical disease impairs its specificity.

Biologic diagnosis is based on two tools that have the largest impact on malaria control today: microscopic examination of Geimsa-stained blood smears and molecular methods such as PCR, ELISA and Immuno Fluorescence Antibody assays, IFA (Spencer *et al*, 1979; Sulzer *et al*, 1969) and in recent years immunochromatographic assay, wich form the basis of commercial malaria rapid diagnostic tools (RDT) available today (Moody and Chiodini, 2002). Both of these biological methods have characteristic strength and limitations (Wongsrichanalai, 2007).

Geimsa microscopy is the most suitable instrument for malaria control because it's inexpensive to perform, able to differentiate malaria species and quantify parasite. However, for microscopy a wide range of poor specificity is reported: poor blood film preparations could generate artifacts that lead to false negative or false positive (McKenzie *et al*, 2003) results (as an example normal blood components such as platelets may confound the diagnosis). Finally, also a well-trained microscopist could make errors in species identification or in parasite density extimation.

Malaria rapid diagnostic tests, sometimes called "dipsticks" or malaria rapid diagnostic devices (MRDDs), assist in the diagnosis of malaria by providing evidence of the presence of malaria parasites in human blood. It consists of a device able to detect a malaria antigen with monoclonal antibody directed against the targeted parasite antigen and impregnated on a test strip. They still have great limit such as their consumption in developing countries or the persistence of the

recognized even antibody even after sucesfull treatment or the rising costs to their implementation. Molecular assays can provide critical information for malaria diagnosis, speciation, and drug resistance, but their cost and resource requirements still limit their application to clinical malaria studies. Today's investments in anti-malarial drug development should be accompanied by the improvement of diagnostic tools and their availability to those living in malarious areas.

Topoisomerase of protozoan *Plasmodium falciparum*

Plasmodium falciparum is a protozoan parasite, one of the species of *Plasmodium* that cause malaria in humans. Protozoan parasites in general are responsible for a wide range of debilitating and fatal diseases that are notoriously difficult to treat. Each year, there are more than 250 million cases of malaria, killing between one and three million people, the majority of whose are young children in sub-Saharan Africa. Rapid onset of resistance to most widely used antimalarial compounds requires continuous evaluation of novel drug targets and development of novel antimalarial drugs (Reguera *et al*, 2006); effective treatment of malaria relies also on sensitive and accurate diagnosis.

TopIB was first decribed from the murine parasite *Plasmodium berrghei* by Riou who purified and characterized the enzyme from infected erytrocytes (Riou *et al*, 1986). Later the gene encoding topoisomerase I in *Plasmodium falciparum* (pfTopIB) has been cloned

and characterized. This enzyme consist of a monomeric protein of 104 kDa corresponding to a peptide of 839 aminoacids, encoded by a 2520 bp open reading frame located on a plasmodial chromosome 5 (Tosh and Kilbey, 1995). This enzyme resembles others topoisomerases, maintaining 42% per cent identity and 64% similarity with the human enzyme. The protein has three structural domains:

- N-terminal domain (134 aa) that is poorly conserved.
- A 500 residues long block of conserved amino acids with high level of homology to the human Core domain.
- C-terminal domain, smaller than the one of the host but with the conserved catalyitic Tyrosine (Tyr 798).

Two stretches of non-repetitive aminoacids insertions are predicted to fall within the core domain but the functional significance of these insertions remains an open question (Cheesman, 2000).

PfTopIB is developmentally regulated during the various stages of the Plasmodium life cycle; the pfTopIB promoter is inactive during the ring parasite form becomic active during the asexual intraerythrocytic cycle (Tosh *et al*, 1999).

By definition, enzymes convert substrate molecules to products with changed chemical or physical characteristics without being affected by the process. Hence, at least theoretically, one enzyme can create indefinite amounts of product provided with sufficient substrates and, consequently, the most sensitive detection of pathogens imaginable would rely on detection of species-specific enzymatic products. The challenge is that only few enzymatic products are readily detectable without the use of sophisticated equipment and even then, most products can be detected only when produced in high numbers.

For clinical relevant identification of pathogens based on species-specific enzymatic activities it is, therefore, necessary to develop new technologies.

Single molecule detection of Topoisomerases activity

Current methods for detection of intracellular topoisomerase I consist of real-time RT-PCR, Western Blotting, Elisa and FISH. They do not detect its activity. Recently has been developed a novel single-molecule detection system (RCA-based tecnique) for the clinically important human topoisomerase IB (Stougaard *et al*, 2009). The detection of hTopI activity using RCA assay fulfills the requirements for simplicity, speed and sensitivity and presents the additional advantage of being suitable for multiplexed system for clinical purposes (Andersen *et al*, 2009). The tecnique is based on a oligonucleotide substrate that self folds in a open dumbell shape (FIG 9A), allowing a single cleavage-ligation event mediated by hTopI to be detected in terms of a single fluorescent RCP (Rolling Circle Product). HtopI is able to cleave at its preferential site on the substrate and then religate it, following its catalitic cycle.

This reaction transforms the open dumbbell-substrate into a closed circle (FIG 9B-I and 9B-II). Since the reaction equilibrium of hTopI is shifted toward religation, the formation of the closed circular product is favored. HTopI-mediated-circularization of the dumbbell substrates is detected using a solid support assay comprising rolling circle DNA synthesis and fluorescent labeling, essentially as described previously

(Lizardi *et al*, 1998). The RCA is initiated from a primer (RCA-primer) attached to a glass surface (FIG 9B-IV) to ensure anchoring of the generated RCPs which are subsequently detected at the single-molecule level by annealing to specific fluorescent labeled probes (detection probes) and microscopic analysis (FIG 9B-V). Each microscopically detected fluorescent spot represents one RCP, which in turn represents one closed circle product.

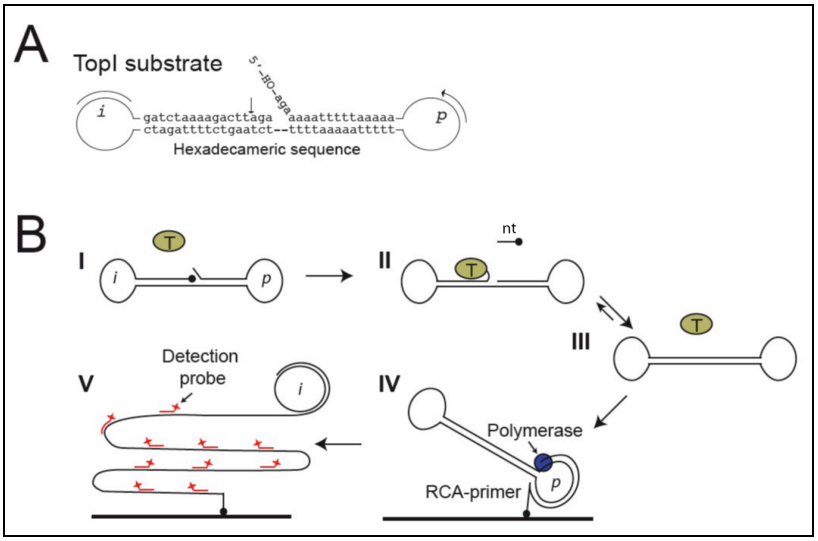

Figure 9. Schematic representation of the RCA-based topoisomerase activity detection. A) Dumbbell substrate B) Set up of the method (Stougaard, 2009).

Hence, since each cleavage-ligation reaction by hTopI generates one closed circle product, the presented setup allows hTopI activity to be detected at the level of single cleavage-ligation events (FIG 9B). The setup is specific and highly sensitive and it has been found to be able to detect hTopI activity at the single cleavage-ligation event level in

purified enzyme fractions but also in crude extracts from yeast (Stougaard *et al,* 2009). The detection limit of approximately 0.1 fmol (10^7 molecules) of purified hTopI in the current crude setup indeed holds promise for the future detection of the hTopI activity level in even very small clinical tissue or cell samples, since the content of hTopI in mammalian cells being estimated to at least 10^5 molecules (Champoux, 1978).

An important inherent property of the presented setup is, at least in theory, the easy adaptability to multiplexed enzyme detection simply by using differently labeled probes for the detection of rolling circle products of different circularized substrates. Infact it has been demonstrated the possible specific detection of three different enzyme activities, hTopI and the two recombinases Flp and Cre in nuclear extracts from human cells one at a time or multiplexed using the rolling circle amplification based single-molecule detection system (Andersen *et al*, 2009).

AIM OF THE PROJECT

Rapid, specific and high-throughput oligonucleotide diagnostic approaches to identify pathogenic diseases are of great importance to medical fields. Direct and sensitive DNA or enzyme detection from samples collected directly from patients may avoid expensive and lengthy traditional assay approaches, which utilize antibodies and cell cultures. The aim of this research project has been to develop a DNA-based biosensor with potential use for future at-point-of-care diagnosis of malaria. The biosensor uses a novel rolling circle amplification approach, already applied for the conversion of a single human topoisomerase I mediated DNA cleavage-ligation event in a product readily detectable using standard fluorescence microscopy (Stougaard *et al*, 2009). The conversion, achieved by topoisomerase I, induces the closure of a nicked DNA dumbbell structure (FIG 9A), followed by hybridization to a primer on a functionalized slide. The circularized substrate is then amplified by rolling circle amplification and the resulting product consists of multiple tandem repeats of the DNA dumbbell substrate that can be subsequently visualized by annealing it with fluorescently labeled probes. Amplification doesn't involve any thermal cycling so each rolling circle product, which gives rise to a single fluorescent signal, corresponds to a single topoisomerase I mediated cleavage-ligation event. Regarding sensitivity, speed, and ease of performance, the RCA assay based on single-molecule product detection is superior than any current state-of-the-art assays using

supercoiled plasmids or radiolabeled oligonucleotides as substrates to detect topoisomerase I activity.

During the project two approaches have been mainly carried out, the first aimed to the development of a specific substrate or conditions for the selective detection of pfTopI; the second one aimed at the increase of the sensitivity of the tecnique.

1) In the first case the RCA set up has been modified to specifically distinguish between hTopI and pfTopI activity, either separately or in a multiplexed detection system. A synthetic gene encoding pfTopI has been cloned and the recombinant protein expressed in and purified from *Saccharomyces cerevisiae.* The activities of the two enzymes have been investigated using the dumbbell substrate (FIG 9; Stougaard *et al*, 2009) and a specific substrate for pfTopI has been developed. The hTopI and pfTopI ability to circularize the substrates has been studied as a function of salt concentration either using the recombinant purified forms, in a cell line extract or in red blood cells extracts.

2) In the second case the fluorescent signals have been made more intense using the RCA primers concentrated on functionalized beads. In detail, the sensitivity of sepharose beads, functionalized with RCA primers (Schopf and Chen, 2010), has been evaluated in comparison with the functionalized slides. The beads have an average diameter of 20-30 μm and can capture hundred of thousand of circularized substrate. This procedure gives sensitivity approximately 100 times higher than the first one, but it must still be optimized to improve the quantification.

MATERIALS AND METHODS

Codon optimization of pfTopI gene

A synthetic gene was produced (GeneArt, Regensburg, Germany) based on the DNA sequence of the P.*falciparum* 3D7 strain pfTopI gene (accession number PFE0520c). Codon usage was optimised for S.*cerevisiae.* The synthetic product was PCR amplified from the production vector using Expand High Fidelity PCR System (Roche, Basel, Switzerland); reactions contained 300 nM each primer forward AP1595 (ATG CAA TCT ATG GAA ATT AA) and reverse AP1597 (TCA TTAGAA AGT GAA GTT CT), 200 µM each dNTP, 2,6 U enzyme mix, 0,5 µL template and 1,5 mM $MgCl_2$ in Expand High Fidelity Buffer, final volume 50 µL.

The thermal profile was 94ºC for 2 min, 5x [94ºC for 15 sec, 45ºC for 30 sec, 60ºC for 4 min], 10x [94ºC for 15 sec, 50ºC for 30 sec, 60ºC for 4 min], 15x [94ºC for 15 sec, 50ºC for 30 sec, 60ºC for 4 min + 5 sec/cycle], 60ºC for 7 min.

Cloning and plasmid purification of synthetic pfTopI gene

The 50 µL PCR reaction was incubated with 1U Taq polymerase (Invitrogen, Carlsbad, California) at 72ºC for 10min to add A-overhang at the 3' ends, and was cloned into the pYES2.1/V5- His-TOPO vector (Invitrogen, Carlsbad, California) according to manufacturers protocol. 2 µL of the cloning reaction was used to

transform 50 µL of E.coli Top10F' cells (Invitrogen, Carlsbad, California) by heatshock according to manufacturers protocol and cells were plated on 2xTY (8g peptone, 5g yeast extract, 2.5g NaCl, 10g agar ddH_2O until 500ml) with ampicillin selection. Liquid cultures for minipreps were set up with 3mL 2xTY and 0,1mg/mL ampicillin, incubated with 200 rpm agitation at 37ºC for 16 hours and plasmids were purified using Qiagen Plasmid Mini Kit (Qiagen, Hilden, Germany) according to manufacturers protocol. DNA pellets were resuspended in 30 µL TE (10 mM Tris, 1 mM EDTA) pH 7,5.

Sequence verification of synthetic pfTopI gene

The sequence of the cloned synthetic gene was verified by sequencing with BigDye Terminator 3.1 (Applied Biosystems, Foster City, California) on an ABI3130 platform using primers AP1600 (AGA AAA AAT CAA ACC TCT ATG) and AP1604 (ATG ATA AGA ACT CTC CAA TTG). Reactions contained 0,17 µL DNA, 2 µL BigDye Terminator, 2 µL BigDye buffer and 250 nM primer in total volume 12 µL. The reactions were run on a thermal cycler with the profile 96ºC for 1 min, 25x [96ºC for 10 sec, 50ºC for 5 sec, 60ºC for 4 min], then 10 µL ddH_2O was added and samples were sequenced by the sequencing core facility at Institute of Molecular Biology (University of Aarhus, Denmark).

Selective growth medium for pYES2.1/V5-His

The expression plasmid (pYES2.1/V5-His) containing the synthetic gene allows transformants to be grown in uracil deficient medium. Raffinose medium without uracil (Raffinose Ura^-) is made with 12g Ura^- dropout, 17g yeast nitrogen base, 50g ammoniumsulfate and 100g raffinose in 10L ddH2O. The medium is autoclaved before use.

Transformation of *S.cerevisiae* with synthetic pfTopoI

The S.*cerevisiae* RS190 strain, which lacks of endogenous TopIB, was used for expression of the synthetic pfTopoI gene. Approximately 20 µL cells were scraped from a petri plate and transferred to 1 mL sterile water and then they were spun down at max speed for 5 seconds; the pellet was resuspended in 1 mL 100 mM LiAc and incubated 5 minutes at 30ºC. The suspension was spun down at max speed for 5 seconds and supernatant was removed. Transformation reagents were added in the following order: 240 µL PEG (50% w/v), 36 µL 1 M LiAc, 25 µL salmon sperm ssDNA (2mg/mL), 5 µL plasmid DNA and 45 µL ddH_2O. The tube was vortexed for 1 minute and incubated at 42ºC for 20 minutes. Cells were spun down at max speed for 10 seconds and supernatant was discarded. The pellet was gently resuspended in 200 µL ddH_2O. The suspension was plated on Ura^- raffinose plates and incubated at 30ºC until colonies were visible.

Large scale pfTopI expression and mechanical lysis

Single colonies from the transformation were used to inoculate 5 mL of raffinose Ura$^-$ medium with 2% glucose and grown at 30 ºC untill OD600 was >1 (2-4 days).

5 mL of culture was used to inoculate each of 8 flasks with 1,5 L raffinose Ura$^-$ medium at an initial OD600 of 0.05, 12 L of culture total. The flasks were incubated at 30 ºC at 200 rpm agitation and 150 mL 20% (w/v) galactose (final 2%) was added when an OD600 of 0.5 was reached. After induction for 18 hours the 12 L culture was spun down in 1 L cups at 4000 rpm at 4ºC C for 15 minutes with gentle braking. The cell pellets were transferred to 50 mL NUNC tubes, spun down at 4000 rpm for 15 minutes and the rest of the supernant removed. The cell pellets were removed from the NUNC tubes and frozen in liquid N_2. Cells were lysed mechanically by blending during immersion in liquid N_2. The frozen lysate was brought to 0ºC and 30 mL 0M Eluition buffer (10 mM Tris pH 7.5, 0.5 mM EDTA, 10% glycerol) was added.

120 mL saturated ammoniumsulfate (Ams) was added to precipitate proteins overnight at 4 ºC. Ams supernatant was removed and protein pellet (300 mL) was spun down in 6 200 mL containers at 10.000 rpm for 30 minutes at 4ºC, and supernatant was discarded. A total of 100 mL 0M Elu with 100µL PMSF and 100 µL DTT (1M) was distributed in the 6 containers, which were placed on ice on a rocking table at 4ºC. The protein pellets were left to resuspend with gentle agitation and 5µL PMSF was added to each container every 15 minutes. The total volume of protein + buffer was determined, and

the suspension was gently diluted in 504 mL 0M Elu corresponding to 42x protein volume (protein 42 pellet was 12mL). Cell debris was removed by vacuum filtering the suspension through 0,65 µm and 0,45 µm filters.

Purification with heparin columns

The crude protein extract was purified on a column containing approximately 2,5g Heparin Sepharose CL-6B material (GE Healthcare, Piscataway, New Jersey). The protein extract was loaded and washed in 0,1M Elu (10 mM Tris pH 7.5, 0.5 mM EDTA, 10% glycerol, 100 mM NaCl) and eluted in 25x2mL fractions with 1M Elu (10 mM Tris pH 7.5, 0.5 mM EDTA, 10% glycerol, 1 M NaCl) and 25x2mL fractions with 2M Elu (10 mM Tris pH 7.5, 0.5 mM EDTA, 10% glycerol, 2 M NaCl). The active fractions (assessed with a relaxation assay) were pooled and diluted to 0,1 M NaCl and loaded on a second heparin column (approx. 2 mL column material). 60x0,5 mL fractions were eluted with a linear NaCl gradient from 0,1 M to 2M Elu, and an additional 20x0,5 mL fractions were eluted with 2 M Elu (80 fractions total). Peak fractions were determined by performing relaxations with 200x diluted protein eluate. Active fractions were added 500 µL 87% glycerol (final concentration 50%) and stored at -20ºC.

Relaxation assay

200 pmol of supercoiled pAD plasmid were incubated with 1 ul of protein fraction in topoisomerase buffer (100 mM Tris pH 7,5, 10 mM EDTA, 50 mM $CaCl_2$, 50 mM $MgCl_2$).

NaCl was added to reach the salt optimum in a final volume of reaction of 20 µl. The reactions were incubated at 37 ºC for 35 minutes, 2 µl 2% SDS and 2 µl Proteinase K (10mg/mL) was added and samples were incubated at 37 ºC for 1 hour. Electrophoresis of the samples was carried out in a 1%(w/v) agarose gel in TBE 1x (96 mM Tris, 91 mM boric acid and 1.9 mM EDTA) at 10 V/cm to display the result.

Nuclear extraction of HEK293T mammalian cells

Human embryonic kidney HEK293T cells were cultured in Dulbecco's Modified Eagle Medium (DMEM) (Invitrogen, Carlsbad, CA, USA) supplemented with 10% fetal bovine serum (Gibco, Carlsbad, CA, USA) and 1% streptomycin/penicillin (Gibco) at 37˚C in a humid atmosphere containing 5% CO_2.

Cells from 2 T75 flasks were collected in 2 NUNC 50 ml tubes and harvested xffor 2 minutes at 2000 rpm. After removal of the medium the cell pellets were resuspended in 1 ml of cold PBS 1x (8 g NaCl, 0.2 g KCl, 1.44 g Na_2HPO_4, 0.24 g KH_2PO_4 in 800 ml of distilled H_2O) in presence of 1 µl of DTT 1M and 2 µl of PMSF.

The cells resuspension were spun down at 2000 rpm for 5 minutes, the supernatant was removed and the pellets were resuspended in 1 ml of cold lysis buffer (0,1% NP40, 10 mM Tris pH 7,9, 10 mM $MgCl_2$,

15 mM NaCl) in presence of 1 µl of DTT 1M and 2 µl of PMSF (Mo *et al*, 2000). The cell resuspension was incubated on ice for 10 minutes and then spun down at 2000 rpm for 5 minutes at 4 ºC. After discarding the supernatant, 200 µl of Nuclear extraction buffer (0,5 M NaCl, 20 mM HEPES pH 7.9, 20 % glycerol) in presence of 1 µl of DTT 1M and 2 µl of PMSF were added to the eppendorf tubes without resuspending the pellet (Hann *et al*, 1998). The tubes were placed on a tilt rotator at 4 ºC for 1 hour. Then the tubes were spun down at 11000 rpm for 10 minutes at 4 ºC and the supernatant containing the nuclear extract was collected into a new tube and put on ice with DTT and PMSF untill use.

Nuclear extraction from blood samples

Non infected and infected (with *Plasmodium falciparum* parasites) blood samples was stored at -20ºC. The samples were thawed in warm water bath and 3 volumes of RBC lysis buffer (Gentra puregene blood kit, Quiagen) were added; the tubes were mixed inverting 10 times and incubated at room temperature for 10 minutes. The cell debris were spun down at 3000 rpm for 30 minutes and the supernatant was discarded. The pellet was washed with 1 ml of PBS (8 g NaCl, 0.2 g KCl, 1.44 g Na_2HPO_4, 0.24 g KH_2PO_4 in 800 ml of distilled H_2O) in presence of 1µl of DTT 1M and 2 µl of PMSF and transferred to an eppendorf tube; then tubes were spun down at 3000 rpm for 5 minutes and the supernatant was discarded.

After extimation of the debris pellet volume, 2 times pellet volume of Nuclear extraction buffer (0,5 M NaCl, 20 mM Hepes ph 7.9, 20 % glycerol) was added, in presence of 1 µl of DTT 1M and 2 µl of PMSF; the cells debris and parasites were disrupted by repeating passage (10 times) through a gauge G25 syringe. The nuclear extraction was carried out for 1 hour, on tilt rotator at 4ºC. The tubes were spun down at 4 ºC for 10 minutes at 13000 rpm; supernatant was collected, without disturbing the pellet, into a new tube, put on ice with DTT and PMSF untill use.

Synthetic DNA substrates, probes, and primers for RCA

Oligonucleotides for construction of the S(TopI) [=ID16], S(FLP) [=ID33] and control ligated circle [=IDA1], the utilized detection probes p(TopI), p(Flp), and p(control circle) and RCA-primer were synthesized by DNA Technology on a model 394 DNA synthesizer from Applied Biosystems. The oligonucleotides representing the dumbbell-substrate [ID16] and the RCA-primer were modified by a 3'- and a 5'-amine group, respectively. For preparatio of the control circle, the control ligase substrate was circularized by T4 ligase, and the resulting ligated circles were purified from a 8% polyacrylamide gel. The concentration of the obtained circles was determined by spectrophotometric measurement.

The sequences of the oligonucleotides are as follows:

- <u>Substrates:</u>

  - S(TopI): 5'-AGAAAAATTT TTAAAAAAAC TGTGAAGATC GCTTATTTTT TTAAAAATTT TTCTAAGTCT TTTAGATCCC TCAATGCTGC

TGCTGTACTA CGATCTAAAA GACTTAGA-AMINE- 3';

- S(Flp): 5'-TCTAGAAAGT ATAGGAACTT CGAACGACTC AGAATGAGGC TCAATCTAAT GGACCCTCAA TGCACATGTT TGGCTCCCAT TCTGAGTCGT TCGAAGTTCC TATACTTT-3';

- S(control ligase substrate): 5'-AGAAAAATTT TTAAAAAAAC TGTGAAGATC GCTTATTTTT TTAAAAATTT TTCTAAGTCT TTTAGATCCC TCAATGCTGC TGCTGTACTA CGATCTAAAA GACTT-3';

- RCA-primer, matching s(TopI), s(FLP) and s(control ligase circle): 5'-AMINE-CCAACCAACC AACCAAATAA GCGATCTTCA CAGT-3';

- Detection probes:

  - p(TopI): 5'-"F"-GTAGTACAGC AGCAGCATTG AGG-3';

  - p(Flp): 5'-"F"-GGAGCCAAAC ATGTGCATTG AGG-3';

  - p(control circle): 5'-"F"- GGCTCTACATGGCGATAGCA-3';

"F" indicates fluorescent labeling, which was Rhodamine, FITC or Cy5.

Coupling of amino oligonucleotides to CodeLink® activated slides

CodeLink® (GE Healthcare) activated slides are designed to covalently immobilize amine-modified DNA oligonucleotides. Slides for RCA were prepared cutting 1 cm^2 of CodeLink® glass and attaching them to an objective glass (superfrost glass slides). A square

was drawed with a PAP-pen that provides a thin film-like green-tinged hydrophobic barrier. A coupling mixture was prepared mixing 0.83 µl of 6x print buffer (29,7 mM NaH_2PO_4, 267 mM Na_2HPO_4, pH 8.5) with 2,5 µl of 10 µM in 5 µl of final volume (5 µl for print each slide). The coupling was carried out over night in a humidity chamber with saturated NaCl at room temperature. Then slides were blocked for 30 minutes using blocking buffer (115 mM Tris- HCl, 50 mM ethanolamine, pH 9) at 50ºC, washed for other 30 minutes in wash buffer 1 (60 mM $Na_3C_6H_5O_7$, 600 mM NaCl, 0,1% SDS) at 50ºC. After washing the slides werelet to air dry and stocked in the dark untill use.

Circularization by purified TopI

The hTopI and pfTopI circularization reactions were carried out in 30 µl reaction volume. Purified proteins were incubated in one case with 0.2 µM dumbbell-substrate [ID16] in standard hTopoI reaction buffer (10 mM Tris-HCl, pH 7.5, 5 mM $CaCl_2$, 5 mM $MgCl_2$, 10 mM DTT, 0.2 µg/µL BSA), for 1 hour at 37 °C. In the other case the proteins were incubated with 0,2 µM of ID16 and 0,2 µM of ID33 in FLP buffer (5 mM Tris-HCl pH 7.5, 2 mM EDTA, 8 mM NaCl, 0.6% beta-mercaptoethanol, 10% PEG6000) for 1 hour at 37 °C. The reactions were supplemented with different NaCl concentration, as stated in results. After incubations the 2 enzymes were heat inactivated at 95°C for 5 minutes and the samples were stored at -80°C.

Circularization in nuclear extracts.

Topoisomerases activity was detected at single molecule level in nuclear HEK293T extracts and red blood cells extracts. In both cases fresh nuclear extracts were incubated with 0,2 uM of ID16 and 0,2 uM ID33 at 37 °C for 1 hour in FLP buffer (5 mM Tris-HCl pH 7.5, 2 mM EDTA, 8 mM NaCl, 0.6% beta-mercaptoethanol, 10% PEG6000) supplemented with different NaCl concentration as stated in the results.

After circularization the samples were heat inactivated at 95°C for 5 minutes. The circularized product were exonuclease digested: the reactions were supplemented with 7 units exonuclease I and 70 units exonuclease III and incubated for 60 min at 37 °C before inactivation for 15 min at 80°C. Samples were then stored at -80°C untill the hybridization.

Solid support amplification

Self hybridization of samples to the primer-printed slides was performed adding 5 µl of each samples in the middle of the idrofobic delimited square; slides were put in a humidity chamber. After 30 minutes at room temperature the slides were washed in wash buffer 2 (0.1 M Tris-HCl, 150 mM NaCl, and 0.3% SDS) for 1 minute and for another minute in wash buffer 3 (0.1 M Tris-HCl, 150 mM NaCl, 0.05% Tween-20). Finally slides were dehydrated for 1 additional minute in 99,9% ethanol and air dried. Rolling circle DNA synthesis was performed for 45 minutes at 37°C in 1x Phi29 buffer supplemented with 0.2µg/µl BSA, 250 µM dNTP, and 1 unit/µL

Phi29 DNA polymerase; slides were incubated in a humidity chambre on a hot plate. The reaction was stopped by washing in wash buffers 2 and 3 for 1 minute each, deydrateted in 99,9% ethanol for 1 minues and air dried. The RCPs were detected by hybridization to 0.17 µM of each of the detection probes in a 2x hybridization buffer (20% formamide, 300 mM NaCl, 30 mM $Na_3C_6H_5O_7$, 5% glycerol) for 30 minutes at 37°C. The slides were washed in wash buffers 2 for 15 minutes and in wash buffer 3 for 5 minutes, dehydrateted in 99,9% ethanol for 1 minute and air died, mounted with 2,5 µl of vectorshield without DAPI and covered with a coverglass.

Slides where analyzed under a 63x objective in a Leica epifluorescence microscope (Stougaard *et al*, 2007) and images recorded with a SenSys CCD-camera operated by the SmartCapture 2 version 2.0 image analysis from digitalscientific (Cambridge, UK).

Quantification of fluorescent RCP

10 nM of control circles were added to the 5 µl samples before the hybridization to slides. The RCA was performed as stated in the solid support section. The obtained pictures were analyzed using the ImageJ software (NIH) and the number of spot were normalized against the number of RCP derived from control circles.

Sepharose beads based RCA

Amine-reactive sepharose beads (GE Healthcare) were removed from one affinity column and immediately suspended in a 1 ml solution of

100% ethanol. 10 µl of solution were transferred to a centrifuge tube and rinsed twice in 100 µl of activation buffer (20 mM K_2HPO_4 pH 8.0).

[For the entire procedure each rinsing step started with a short vortexing to resuspend the beads follone by 10 seconds of centrifugation; the tubes were rotating of 180° and centrifuged again].

10 µl of solution were discarded and the passage was repeated untill removing all the solution. After the last removal 2.5 µM of RCA primer was added in 100 µl of activation buffer. The beads were vortexed to resuspend them and placed on a tilt rotator for 1 hour. The beads were rinsed twice in 100 µl of deactivation buffer (0,5 % ethanolammine, 0,5 M naCl, pH 8.3) and left on tilt rotator for 2 hours. Then they were rinsed twice in storage buffer (50 mM Tri-HCl, 0,02 % Tween-20, 0,02 % SodiumAzide, pH 8). Following these passages the beads became functionalized wit the RCA primer and could be stored at 4°C untill use.

For the hybridization 10 µl of functionalized beads were blocked in 100 µl of blocking buffer (1x PBS, 0,1 % BSA, 50 µg/ml dI/dC) in 200 µl eppendorf tubes. The beads were rinsed one time in blocking buffer and left on a tilt rotator for 6 hours. Then they were rinsed twice in 1x Phi29 buffer and 5 µl of the circularized samples were added with blocking buffer in a finale volume of 100 µl; tubes were beate at 95°C for 5 minutes vortexing during the heat procedure, then they were transferred at 55°C at 1200 rpm for 5 minutes and finally placed on a tilt rotator to allow the self hybridization to procede overnight.

After the hybridization the beads were rinsed three times in 1x Phi29

buffer.

RCA was performed in 10 µl of final volume mixing 3,2 µl of 5x Phi29 buffer, 1,6 µl of 1% BSA, 1,28 µl of 10 mM dNTPs and 0,64 µl of 10 U/ µl Phi29 polymerase; tubes were placed on a thermal shaker at 1200rpm for 3 hours at 37 °C. Following extension beads were rinsed twice in 1x PBS and 0,17 µM of each fluorecent probes were added, tubes were left on a tilt rotator to react overnight. Then they were rinsed twice in storage buffer and resuspended in 50 µl of storage buffer. The visualization was carried out at the Leica microscope in the same way reported for the slides.

RESULTS

HTopI and pfTopI activities have a different salt dependence

The experimental setup for single-molecule detection of the cleavage-ligation activity of hTopI and pfTopI relies on a DNA substrate (referred as "dumbbell-substrate" in the following) composed of a short single-stranded oligonucleotide, which spontaneously folds into a double looped dumbbell-shaped structure, as shown in Figure 9A.
PfTopI is able to cleave the classical hexadecameric sequence (Bonven *et al*, 1985) that contains the preferred cleavage site for most nuclear type IB topoisomerases. Figure 10 shows the dumbbell substrate that is composed of a short single-stranded oligonucleotide, which spontaneously folds into a double-looped dumbbell-shaped structure.

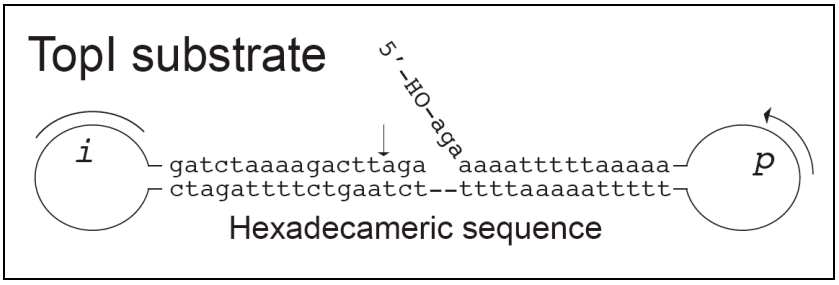

Figure 10. Schematic representation of the dumbbell substrate.

Cleavage of the substrate by pfTopI (but also hTopI) occurs three bases upstream of the oligonucleotide 3'end, resulting in the

temporary covalent attachment of the enzyme and dissociation of the released three nucleotides (nt) fragment (figure 9B-I). This allows the 5'overhang of the substrate, designed to match the non-cleaved strand of the stem sequence, to fill in the generated gap and bring the 5'hydroxyl group in position for TopI mediated ligation (figure 9B-II). As a result, TopI cleavage-ligation activity on the dumbbell substrate generates a closed single-stranded DNA circle (figure 9B-III). To minimize non specific circularization events by DNA ligases, the 3'end of the dumbbell substrate is blocked with a 3'amine group, which does not prevent the TopI catalysis (Stougaard *et al*, 2009).

The TopI mediated circularization of the dumbbell substrates is detected using a solid support assay. Briefly, the circularized substrates hybridize with an oligonucleotide sequence (RCA-primer) attached to a glass surface to ensure anchoring of the generated rolling circle products (RCPs; Figure 9B-IV) generated by the PHI29 polymerase. RCPs are subsequently detected at the single-molecule level by annealing them to specific fluorescent-labeled probes (detection probes) and microscopic analysis (Figure 9B-V).

Each microscopically detected fluorescent spot represents one RCP, which in turn represents one closed circle product (Lizardi *et al*, 1998). Hence, since each cleavage-ligation reaction by TopI generates one closed circle product, the presented setup allows, in principle, TopI activity to be detected at the level of single cleavage-ligation events.

The activity of the two purified enzymes has been assessed as function of the NaCl concentration (FIG 11). Three µl of each enzyme have been incubated with the ID16 substrate (dumbbell substrate) to allow

the circularization at different NaCl concentration. After 1 hour of incubation, the samples have been heat inactivated in order to stop the enzyme's reactions. The circularized samples have been hybridized with the primer-functionalized slides and the RCA has been performed as described. Figure 11 shows selected microscopic pictures of each slide. The pictures demonstrate that eiher hTopI or pfTopI are able to cicularize the dumbbell substrate as evident from the red fluorescents spots presents in each panels which represent one RCP product amplified after the enzyme's circularization. HTopI circularizes the substrate up to 400 mM NaCl (panel IX) while pfTopI shows evident fluorescent signals also at 500 mM NaCl (panel XII). The difference is better shown in the two magnifications reported in panel XIII, that represents a magnification of hTopI activity at 400mM NaCl and in panel XIV, that represents a magnification of pfTopI activity at 500 mM NaCl.

For hTopI there are only few fluorescent spots at 400mM NaCl while incubating ID16 substrate with pfTopI gives rise to a lot of red fluorescent signals also at 500 mM NaCl. This different salt tolerance may enable to distinguish them also in biological samples.

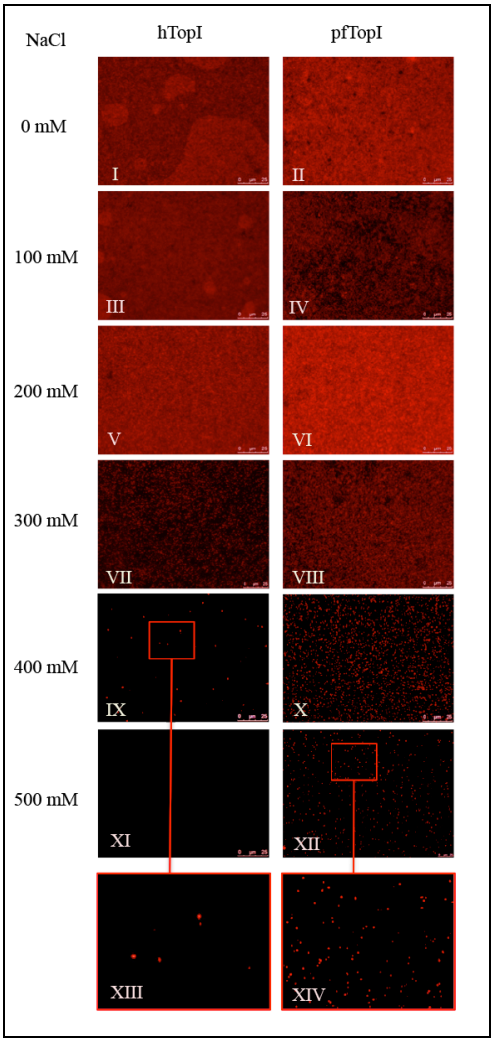

Figure 11. Activity of purified hTopI and pfTopI measured using the dumbbell substrate (ID16) as function of salt concentration. Red fluorescent spots represents one cleavage-ligation event mediated by the topoisomerases.

The activities of htopI and pfTopI differ in salt tolerance in mammalian cell extracts

Most DNA-modifying enzymes require divalent cations for activity, while all topoisomerases I work well in the absence of any cofactors (Champoux, 1994). Hence, false positive signals caused by unspecific enzymatic activities present in cell extracts are likely to be avoided simply by chelating divalent cations adding an excess of EDTA to the reaction mixtures containing crude cell extracts.

In order to assess the NaCl tolerance of both topoisomerases in cell extracts, two T75 flasks of HEK293T cells have been grown and a nucler extracts have been made as reported in literature (Mo *et al*, 2000). The extracts have been incubated with the ID16 substrate in standard Tris-EDTA buffer at different salt concentrations and hTopI or pfTopI have been added. The circularization has been carried out and the RCA signals have been visualized using a fluorescence microscope. Figure 12 shows in the first column (panels I, IV, VII and X) the single molecule assay performed using only the nuclear cell extracts. The second and the third columns (panels II, V, VIII ad XI; panels III, VI, IX, XII) represent signals obtained from the same nuclear extract but after the addition of purified hTopI or pfTopI respectively.

As shown in figure 12 the constitutively expressed hTopI in the extracts has a salt tolerance comparable to the recombinant purified enzyme, with few signals present up to 400 mM NaCl. Addition of hTopI increase the number of signals (FIG 12, compare panel I with

panel II) but any signal is observed at 500 mM NaCl, because both the endogenous and the recombinant hTopI can't circularize the substrate at 500 mM NaCl.

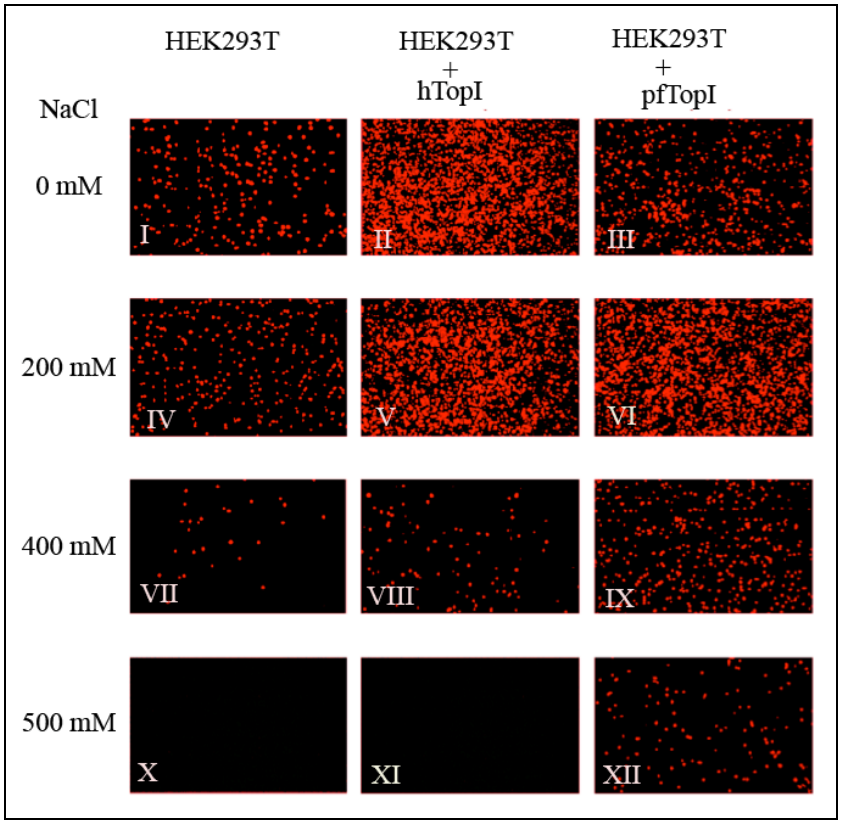

Figure 12. Activities of hTopI and pfTopI in mammalian cell extract. **Panels I, IV, VII and X:** endogenous hTopI activity. **Panels II, V, VIII and XI**: activity of the endogenous hTopI in presence of recombinant purified hTopI added to the extracts. **Panels III, VI, IX and XII**: activity of the endogenous hTopI in presence of recombinant purified pfTopI added to the extracts.

Instead, when pfTopI is added to the extracts it's possible to detect fluorescent spots also at the maximum salt concentration used (FIG 12, compare panels X and XI with panel XII).

This experiment demonstrates that the activity of the hTopI and pfTopI enzymes can be detected well at the single molecule level also in crude biological samples and confirms that the activity of the two enzymes is different at the salt concentrations used as already shown by the experiment made using the recombinant purified forms.

TopIB's detection in human blood extracts

Life cycle of *Plasmodium falciparum* has an erythrocytic stage in the human host, so it's possible to find parasites both in red blood cells and in blood serum, because during their growth the parasites cause the break of the eritrocytes permitting them to infect new cells. Diagnosis of malaria relies in the identification of parasites in the blood. In this thesis the single molecule approach has been used to detect pfTopI activity directly from infected patient's blood.

Infected and non infected blood samples have been treated to extract the nuclear content of the blood cells and of the parasites present in the blood. Nuclear extracts have been incubated with ID16 substrate at different salt concentration and the RCA has been carried out.

The extracts have been used to carry out also a relaxation assay (FIG 13) in order to show how the current state-of-the-art assays (such as relaxation assays) used to detect TopI's activity is not enough sensitive with crude biological samples. Figure 13 shows a typical DNA relaxation assay in which a purified supercoiled (SC) plasmid is

used as substrate. Incubation with TopI leads to the conversion of the high-mobility supercoiled plasmid (FIG 13, marked as SC) to gel-electrophoretic retarded relaxed forms (R); the bands between the SC and the R forms represent topoisomers, molecules of the plasmid with the same molecular weight but with different electrophoretic mobility, that run differently due to their compacteness. Following incubation with blood extracts, the conversion of supercoiled plasmids to relaxed forms has been assayed separating reaction products in a 1% agarose gel prior to visualization by EtBr staining. Figure 13 shows that DNA relaxation is less sensitive than the RCA-based assay (FIG 14) because it converts supercoiled DNA to relaxed form only up to 200 mM NaCl, either in the uninfected or in infected samples. Moreover, the experiment carried out with the infected blood extract shows a lower topoisomerases activity likely due to the lower extraction's efficiency of the nuclear content.

It's remarkable to note that this kind of assay can't provide information concerning the variability of topoisomerases activity in different cell extracts. As shown in figure 14, the uninfected blood extracts has a NaCl profile different from the infected ones. Infected blood extracts exibit some signals also at 400 mM NaCl (FIG 14, panels XIX and XX) while the hTopI in the uninfected human blood sample stop to give signals at 300 mM NaCl (FIG 14, compare panel XVII and XVIII with panel XIX and XX).

Salt tolerance in blood extracts is different from the one identified in the experiments performed using purified enzymes or HEK293T extracts, likely due to the low concentration of topoisomerases that has been extracted from the blood.

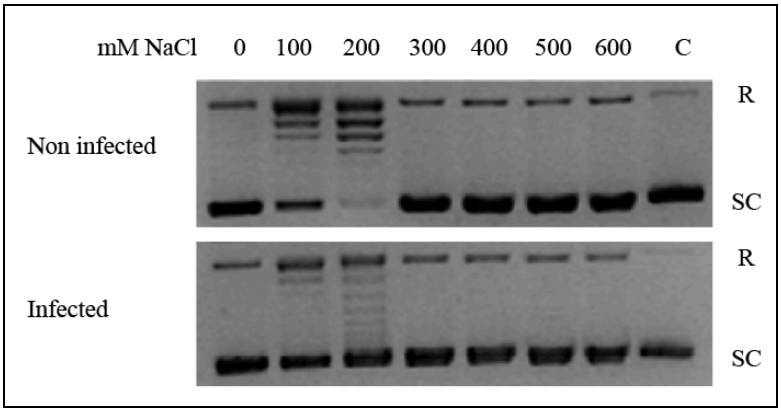

Figure 13. Relaxation assay with non infected and infected blood extracts at increasing salt concentrations.

The experiment has been repeated twice using the same blood samples in order to verify the reproducibility.

The presence of signals at 400 mM NaCl in the infected blood is explained by the presence of pfTopI enzyme coming from parasites. Infact it has been already demonstrated that the recombinant pfTopI has a salt tolerance higher than hTopI.

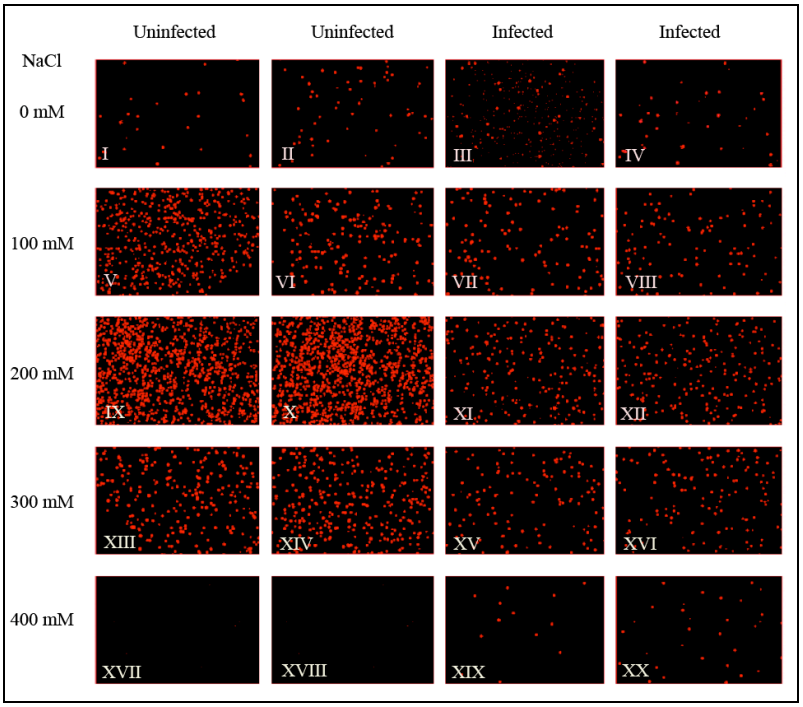

Figure 14. Salt titration of hTopI and pfTopI activities in uninfected and infected blood extracts.

Identification of a specific substrate for pfTopI

The selection of a DNA oligonucleotide substrate, that can be specifically circularized by pfTopI, may permit the specific detection of pfTopI activity in presence of endogenous human topoisomerase, without affecting the assay's sensitivity. To address this possibility, purified pfTopI has been incubated with three different substrates: sCre, sFlp (ID33), and sTopI (ID16), the last one at two different salt

concentration. SCre and sFlp are substrates previously designed to detect the activity of the site-specific recombinases Cre and Flp (FIG 15; Andersen *et al*, 2009).

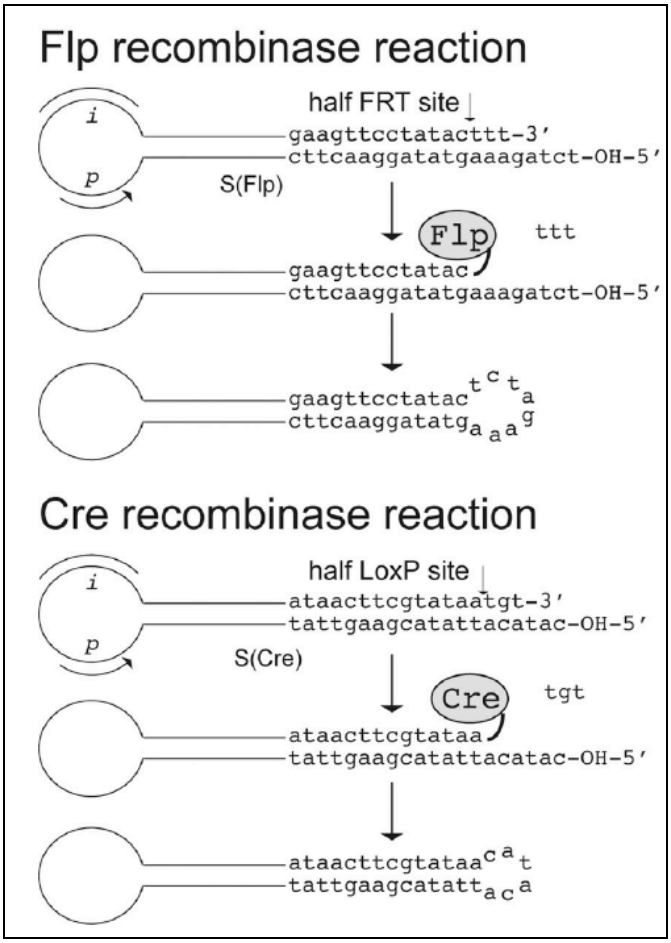

Figure 15. Schematic representation of the solid support RCA-based Flp and CRE activity detection assay.

Flp and Cre are two recombinases that use the basic TopI cleavage-ligation mechanism (Hansen *et al*, 2003) to mediate highly controllable and conservative recombination between two specific sites (i.e the FRT site for Flp19 and LoxP site for Cre20).

SFlp and sCre have been designed to fold into single-looped structures having a sequence matching a half of the FRT-site and a half of the LoxP site, respectively (FIG 15). Both Flp and Cre act in a strictly sequence specific manner with the half FRT site being the minimal cleavage-ligation substrate for FLP (Quian *et al*, 1992) and the half LoxP site being the minimal cleavage-ligation substrate for Cre (Mack et al, 1992). The single loops contain the identifier element (i) and the primer hybridization sequence (p). The Flp and Cre cleavages, at the sites indicated by the arrows (FIG 15), lead to the formation of a covalent cleavage intermediate and to the dissociation of a three-nucleotide generated during cleavage. The cleavage is followed by the ligation of the 5'hydroxyl end to their specific substrate forming a closed DNA circle. As for TopI the reaction equilibrium is shifted toward the religation favoring the formation of circular products. Unspecific cleavage of sFlp or sCre by hTopI has been prevented including an insufficient length of the double-stranded DNA downstream to the cleavage site in these substrates. Infact, although hTopI cleaves DNA in a rather sequence independent manner (Andersen *et al,* 1985; Champoux, 1994), it requires a six base pairs stretch of double-stranded DNA spanning positions 6-11 downstream to the cleavage site (Christiansen *et al*, 1993).

Purified pfTopI enzyme has been incubated with each of these three substrates (sFlp, sCre and sTopI) and the products analysed using the

RCA based detection system. The primer sequence (p), used to attach the substrates (FIG 9 and FIG 15) after the circulariziation, is the same for all the three substrates in order to ensure equal primer annealing efficiency (FIG 16). The microscopic images obtained in the RCA assays cover a random selected area of approximately 0.1 mm^2 out of a total reaction surface of 3x3 mm^2. The concentration of closed circles captured on the surface may vary to a certain extent from one area to another of the same microscopic slide, implying that individual images do not give a precise quantitative estimation of the TopI's activity present in a given sample. In order to obtain more quantitative assay conditions a fixed amount (10 nM) of a gel purified closed control circle has been added to each reaction mixture before loading the sample on the microscopic slide. The circles have the same size of the TopI circularized product and the same nucleotide sequence except for the identifier element that permits the identification through the use of a specific fluorescent probes, to distinguish between them and the circularized products of TopI. As evident from figure 16, pfTopI is able to convert all the substrates to closed circles, readibly detectable in the RCA-based biosensor setup. On the contrary, as already reported, hTopI is not able to convert sFlp and sCre (Andersen *et al*, 2009).

Each column in figure 16 shows the number of the fluorescent signals normalized using the control circles. The sFlp substrate appears to be the most efficiently used by pfTopI (FIG 16, second column) and has been selected to specifically detect pfTopI activity in the RCA setup.

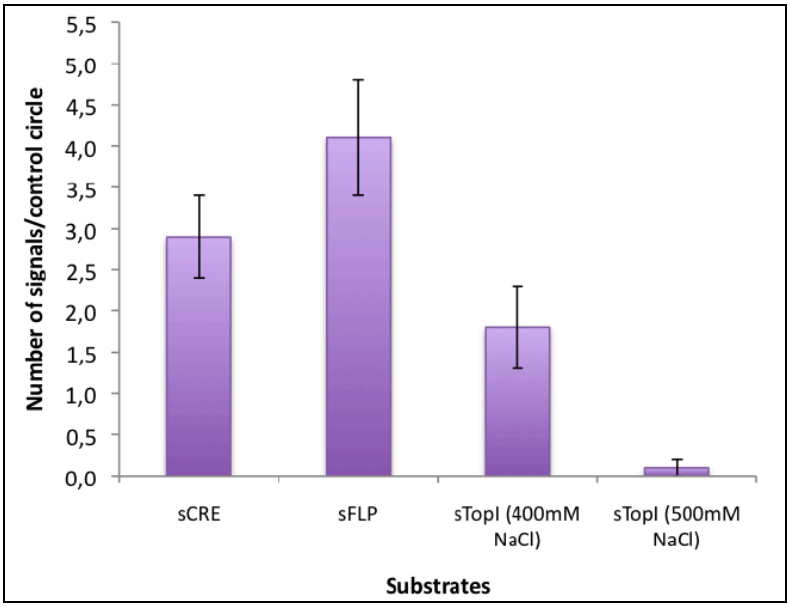

Figure 16. PfTopI substrate specificity. Each graph represents the number of quantified fluorescent signals (as result of pfTopI activity) as function of the substrates used.

PfTopI has a strong preference of sFlp at 200 mM NaCl

The previous result shows that pfTopI is able to process the usual single molecule oligonucleotide substrate also at high ionic strenght. In order to use sFlp as specific substrate for pfTopI (and build a multiplexed detection assay) the salt titration of pfTopI with this substrate has been carried out. Figure 17 shows the activity of pfTopI circularizing the FLP substrate as function of salt concentration. Three µl of purified pfTopI have been incubated with the sFlp substrate

(ID33) at different salt concentration and following the circularization the reactions products have been spotted on the slides together with the control circles (IDA1). The RCA has been performed using two different fluorescent probes to identify both the amplified ID33 substrate and the amplified IDA1 substrate. The microscopic pictures have been taken and imported in the ImageJ software that allows a quantification of the signals. The green spots (from sFlp) observed in twelve randomly selected microscopic images have been quantified and normalized to the number of the blue spots obtained from control circles, IDA1.

It's important to note that the RCA primer hybridization sequence (marked "p" in figures 9 and 15) is identical in the control circle and in the sFlp, so it seems reasonable to assume that the frequency of each of the two DNA species, captured on the individual areas of the microscopic slide, is identical. In figure 17 are represented the pictures of the salt titration. In blue there are the spots coming from the amplification of the control circles (IDA1), which have been hybridized with a Cy5 coupled oligonucleotide probe, in green there are the signals that represent the activity of pfTopI using the ID33 substrate, hybridized with a FITC coupled oligonucletide probe. As evident from the pictures and from the graph obtained after the ImageJ quantification and normalization, pfTopI recognizes ID33 substrate having the maximum efficiency at 200 mM NaCl.

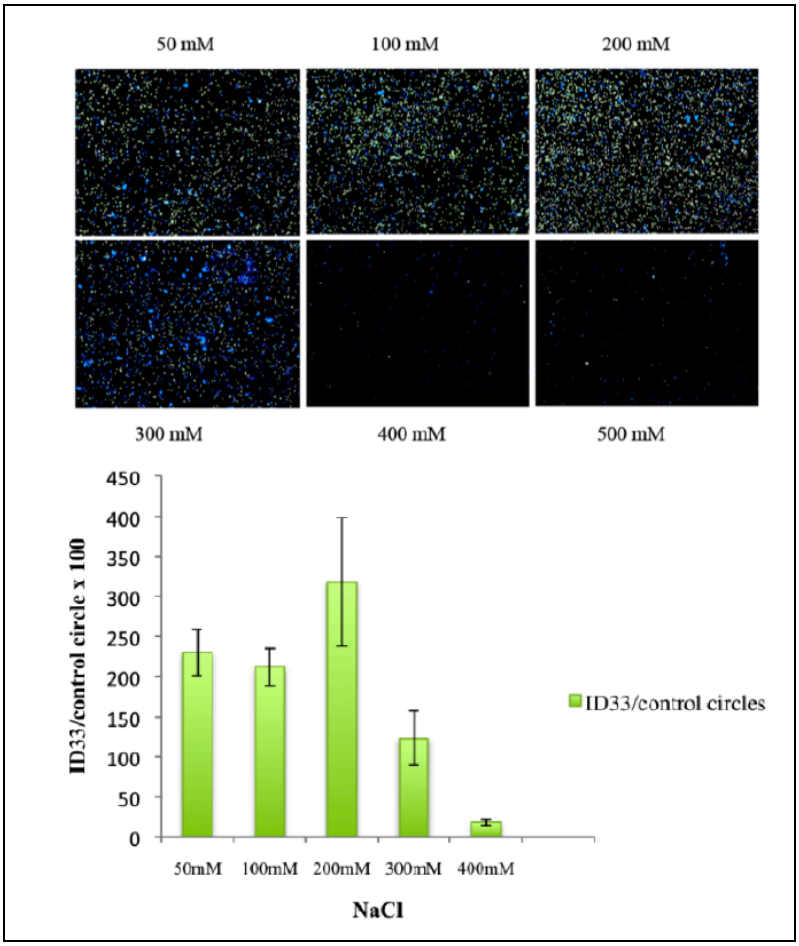

Figure 17. Salt titration and quantification of pfTopI activity using ID33 substrate.

Multiplexed detection of hTopI and pfTopI in mammalian cells extract

A specific biosensor for diagnosis of parasite's disease must efficiently work in crude biological samples. The possibility to use ID33 to detect pfTopI activity in human cell extracts has been tested using the HEK293T cell line. Nuclear extracts have been incubated with both ID16 (to detect hTopI) and ID33 (to detect pfTopI) and three µl of purified recombinant pfTopI have been added in order to mimic an "infected" condition.

After circularization, the samples have been spotted on the slides surface together with 10 nM of control circles (IDA1), to allow a quantification of the ID16/ID33 signals. After the RCA amplification made by the PHY29 polymerase, the RCP products have been hybridized with three different fluorescent probes to distinguish all of them separetely. The "p" element has the same sequence in all the three substrates, so the hybridization to the RCA primer and the consequent amplification is absolutely random, but, in principle, with the same efficiency for all the circularized DNA samples. The assay has been carried out using different salt concentration and twelve pictures for each microspic slide has been taken and the quantification performed as described.

Figure 18 shows some selected microscopic pictures of the salt titration: in absence of spike-in pfTopI (images at the left) it's possible to see only red spots from ID16 amplified product, produced by hTopI and blue spots from amplified control circles, IDA1.

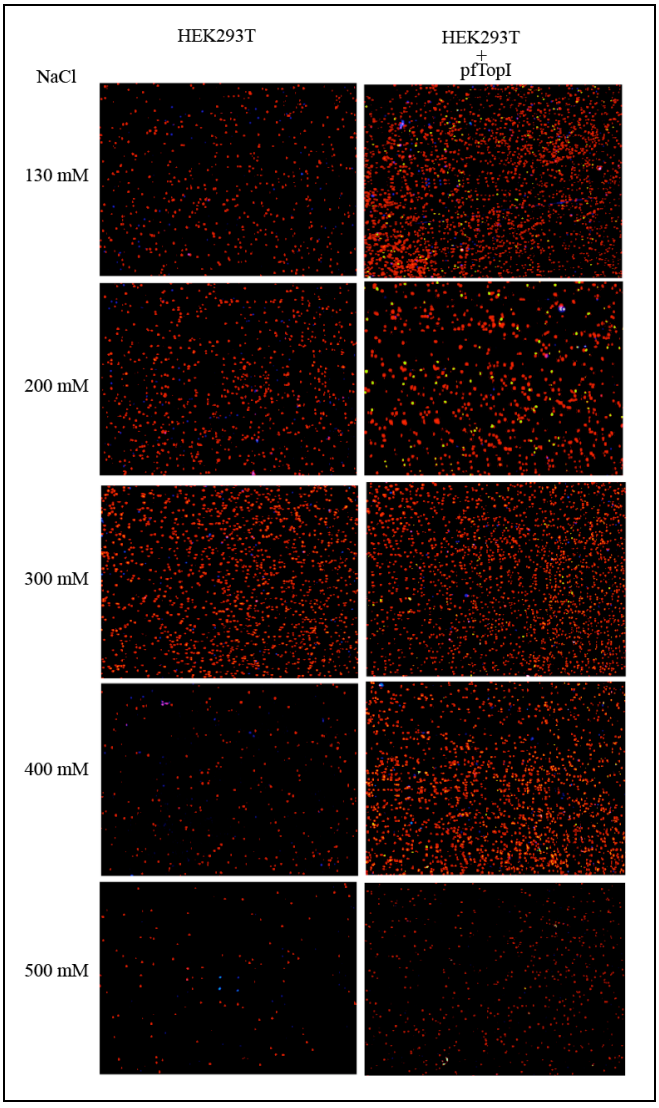

Figure 18. Multiplexed detection of hTopI and pfTopI activity in HEK293T cells extract.

In the images at the right are present also green signals due to the ID33's amplified product. The green signals are present only when pfTopI is added to the reaction, confirming that it's the only enzyme able to recognize sFlp in this assay condition. The salt titration confirms that the salt optimum for pfTopI activity recognizing ID33 substrate is 200 mM. The quantification of these signals is shown in figure 19.

The upper graph shows the intensity of the ID16 amplified products in the HEK293T extract normalized over the control circle (IDA1). In this case no ID33 products are present and the salt optimum is 200 mM NaCl, confirming the result reported in figure 12. The lower graph shows the intensity of ID16 and ID33 in the spike-in pfTopI HEK293T extract, normalized over the IDA1 signals. For both substrates, the salt optimum is 200 mM NaCl.

The number of amplified ID16 signals is higher when pfTopI is added to the extracts because this substrate can be circularized from both the endogenous hTopI and the added recombinant pfTopI. It's important to note that in these assay conditions there are signals coming from hTopI also at 500 mM NaCl, which increase when pfTopI is added (compare the number of ID16 red signals in the upper and the lower graph of figure 19). This result seems to be inconsistent with the previous result (FIG 12) showing the absence of pfTopI activity at 500 mM NaCl. However in that case one µl of extract has been used whilst three µl of extract have been used for all the experiments carried out after the identification of the specific substrate for pfTopI.

The variability highlights the importance to have a specific substrate, since in *vivo* the salt condition may vary from one sample to another one.

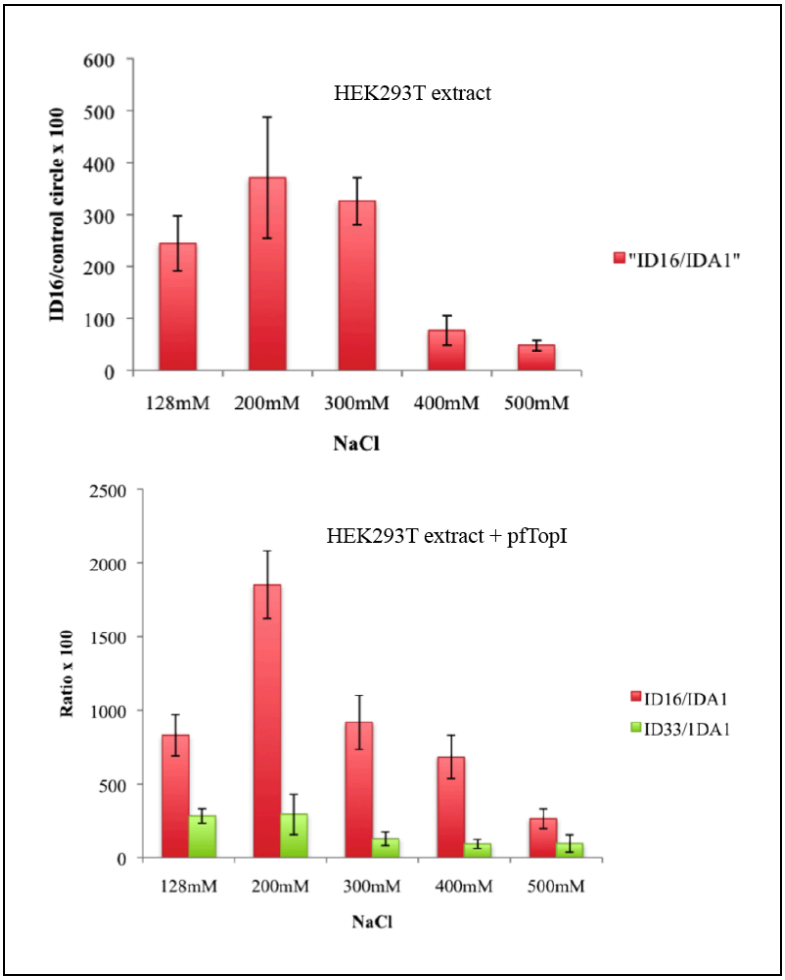

Figure 19. Quantification of amplified ID16 and ID33 in cells extracts. **Upper graph**: normalization of ID16/IDA1 in HEK293T extract; **lower graph**: normalization of ID16/IDA1 and ID33/IDA1 in HEK293T in which pfTopI has been added.

The multiplexed detection experiment at the salt optimum has been repeated to confirm that, in HEK293T's extracts, signals representing hTopI activity (red spots) and due to the control circles (blue spots) are detectable, whilst addition of pfTopI gives rise to specific pfTopI's signals coming from the amplified ID33 and to an increase of the number of red spots (FIG 20, panel II and the magnification in panel IV).

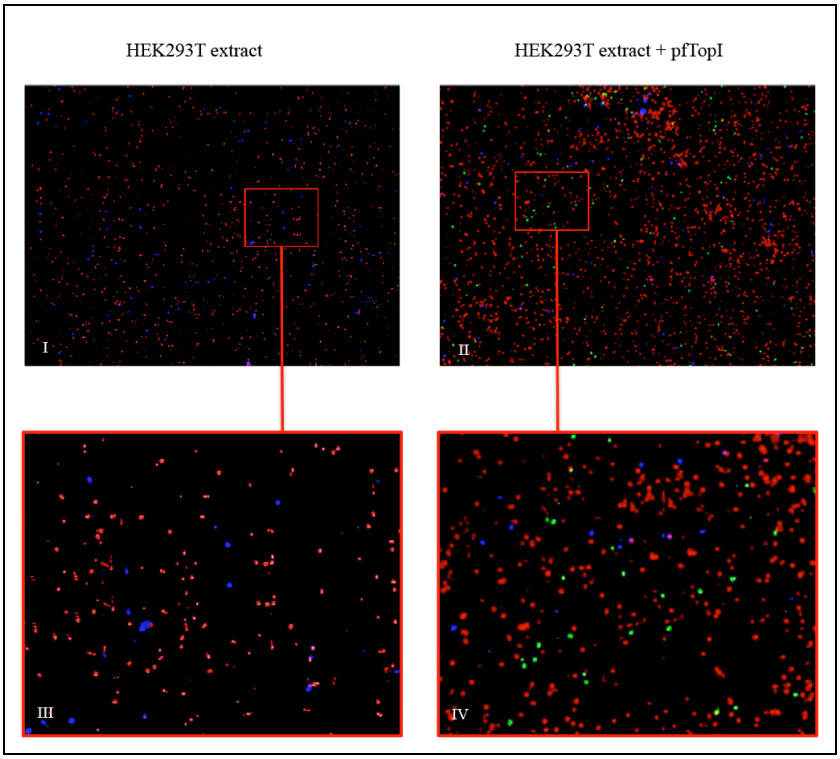

Figure 20. Multiplexed detection of hTopI and pfTopI activities in HEK293T extract at the salt optimum condition. Red = dumbbell substrate's amplified product; blue = control circles; green ID33 (sFLP) amplified product. Panel III and IV = magnification of panel I and II respectively.

Multiplexed detection of hTopI and pfTopI in blood cells extracts

The RCA experiment with the ID16 and ID33 substrates have been carried out also in extracts from either non-infected or *Plasmodium falciparum* infected human blood. In this case the fluorescent probes used to hybridize with the "i" element are green for the spots coming from the amplification of ID16 substrate, red for the ID33 substrate and blue for the control circle (FIG 21).

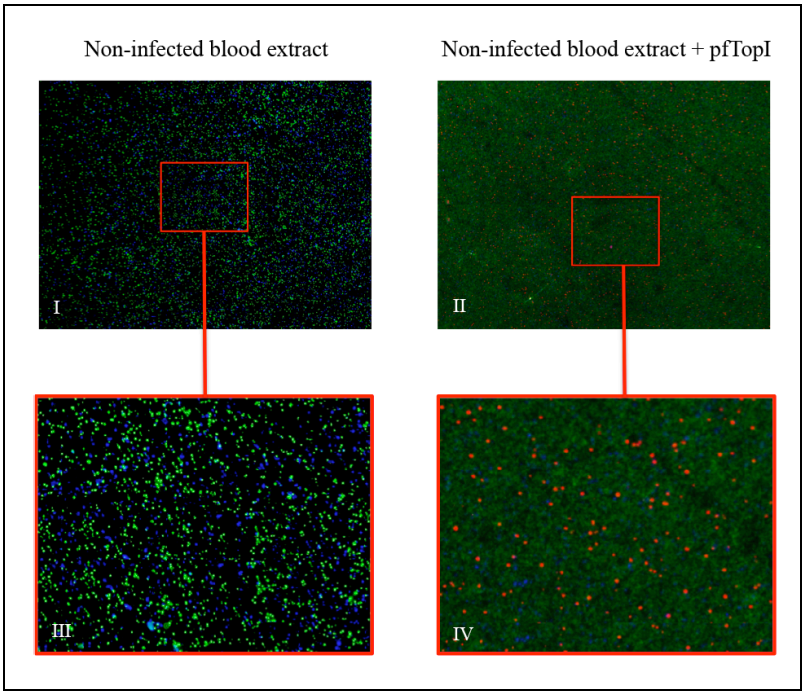

Figure 21. Single molecule detection of hTopI and pfTopI activities in non infected blood extract. **Panel I**: green spots =, blue spots = control circles. **Panel II** : green spots = amplified ID16 product circularized by hTopI and pfTopI; red spots = amplified ID33 products circularized by pfTopI added to the non infected blood extract. **Panel III and panel IV**: magnifications of panel I and panel II respectively.

The non-infected blood has been used as a control in order to confirm the successfull extraction of the cells content and to mimic an infected situation adding the recombinant purified pfTopI.

Figure 21 shows two representative pictures for the single molecule experiment carried out with the non-infected blood extracts, at the salt optimum concentration of 200 mM NaCl. Panel I exhibits the spots that represent the amplification of dumbbell substrate, circularized by hTopI present in the blood cells. In the magnification (panel III) it's possible to identify also the blue spots that represent the control circles. No red signals are present in the slides confirming that the ID33 substrate can't be circularized in the non-infected blood extracts. Panel II and IV show a representative picture and a magnification respectively of the non-infected blood samples in which purified pfTopI has been added. In panel IV several red spots can be identified demonstrating that pfTopI maintains its activity (circularizing specifically ID33 substrate) also in blood cells extracts. The number of green spots is increased because the added pfTopI is able to circularize also the ID16 substrate.

The experiment has been carried out also in *Plasmodium falciparum* infected blood samples from a patient with malaria (FIG 22). The extracts have been incubated with both substrates and the RCA carried out as described. Figure 22 shows one representative picture of the experiment performed at the salt optimum of 200 mM NaCl.

Panel I and its magnification panel II show that few red signals are present in a "carpet" of green spots. The low number of signals specifically produced by pfTopI it's likely due to the low concentration of parasites in the blood's patient.

This experiment unambiguously demonstrate that it's possible to detect the activity of pfTopI in erythrocites infected by P. *falciparum*.

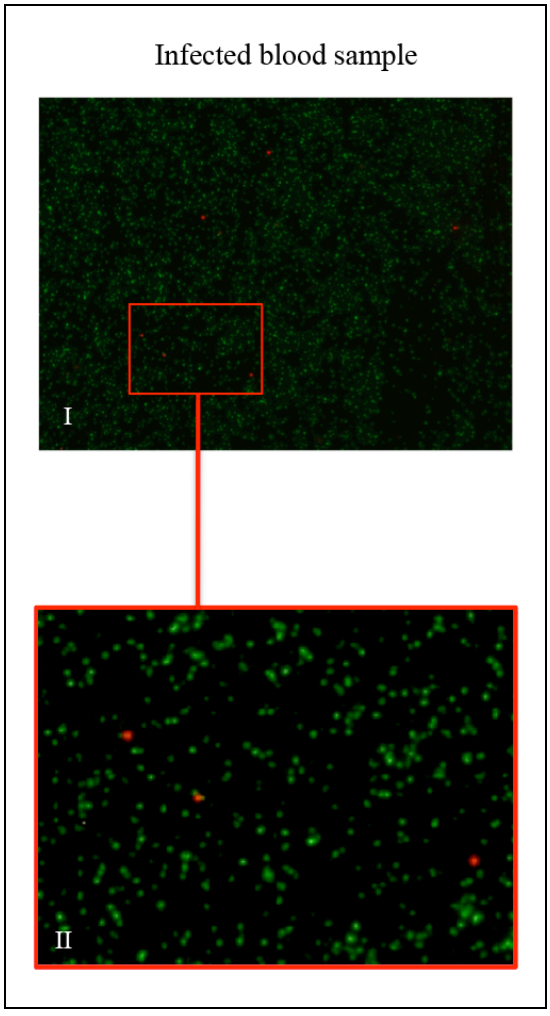

Figure 22. Multiplexed detection of hTopI and pfTopI activities in *Plasmodium falciparum* infected blood sample. Green spots: HtopoI activity. Red spots: pfTopI activity.

Increased sensitivity of RCA based assay using sepharose beads

The experiment of figure 22 unambigously demonstrates the ability of the RCA approach to detect a signal from pfTopI present in blood sample infected by P. *falciparum*. Nevertheless just few signals are observed because the RCA primer is random functionalized on to the glass surface with a consequent spreading of the fluorescent signals coming from the rolling circle products. One possible way to concentrate the signals is to capture the circularized substrates on small beads having an average diameter of 20-30 μm, functionalized with the RCA primers. The beads infact can capture hundred of thousand of circularized substrates leading to an increase of the sensitivity. Recently a similar approach has been used for the sensitive and efficient identification of viral or bacterial DNA avoiding the noise and the contamination of a standard PCR method (Schopf *et al*, 2008; Schopf and Chen, 2009). This setup allows DNA detection in which single target molecules can be imaged directly after RCA. No complicated instruments are required for this assay and the estimated limit of detection is approximately one amol. The setup has been adapted to the single-molecule detection of TopI in order to verify if it's possible to increase the sensitivity of the tecnique. Briefly, amine-reactive sepharose beads have been removed from one affinity column and immediately functionalized with the same RCA primer used for all the experiments described in this thesis. After this step, the hybridization with the circularized sample has been performed and the RCA has been carried out as previously described.

To assess the beads sensitivity, different concentration of control circles have been used to perform an RCA assay using either the sepharose beads or the amino-coupled primer slides. In these cases the RCP have been visualized using a green fluorescent probe (FIG 23).

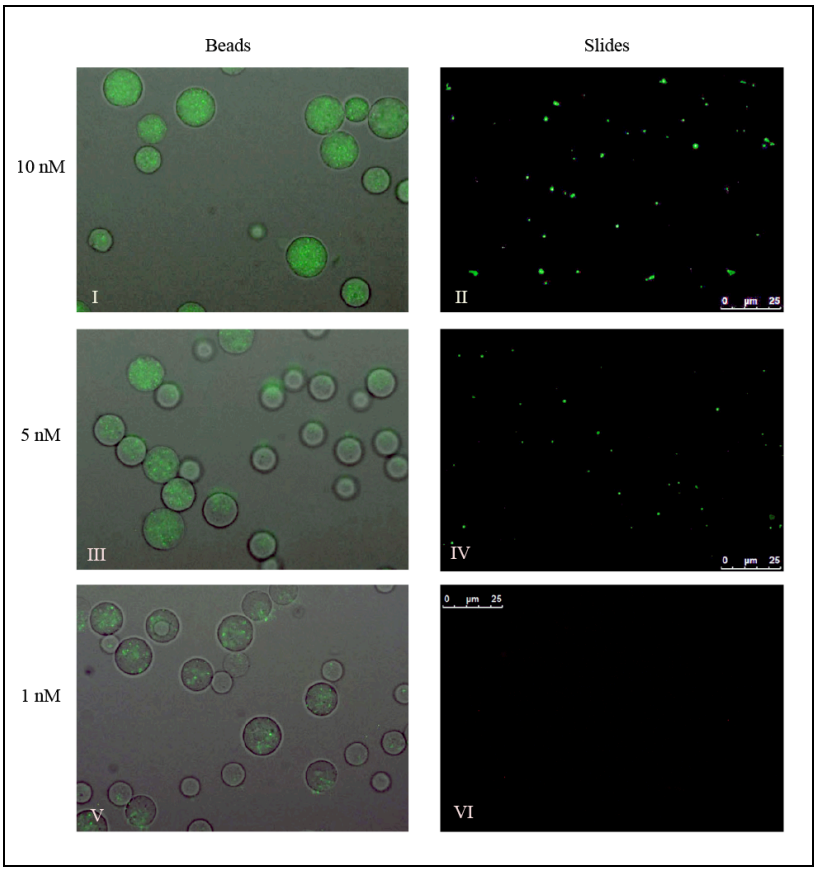

Figure 23. Beads sensitivity. Panels at the left: pictures of the beads at three different control circles concentrations. Panels at the right: comparison with the slides-based RCA.

As evident in figure 23 the number of green spots onto the beads is detectable up to one nM (FIG 23, panel V) while the slides, at this control circle's concentration used, don't give any signal (FIG 23, compare panel IV and VI).

The beads have been also tested using the circularized samples coming from non-infected blood where purified pfTopI has been added (samples used for the experiment shown in figure 21). Figure 24 shows that the beads are covered by green spots that represent the activity of hTopI and red spots that represesent the activity of pfTopI. The same experiment has been carried out diluiting 10 times the sample. Many signals are still detectable (FIG 24, right).

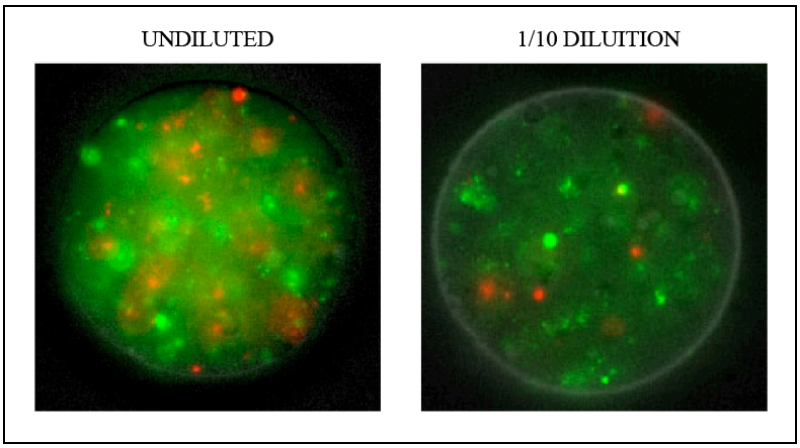

Figure 24. Multiplexed detection of hTopI and pfTopI on to the beads surface. Green fluorescence = ID16 amplified products; red fluorescence = ID33 amplified products.

This result holds the promising possibility to perform the multiplex detection of different enzymes suggesting the increased sensitivity of the beads setup. Moreover, it indicates that the new set up is highly

sensitive and may be used, in the near future, to detect pfTopI also in samples containing low parasite's concentration (saliva from malaria-sick patients).

DISCUSSION AND FUTURE PERSPECTIVES

The results demonstrate the specific and sensitive detection of malaria in clinical relevant samples visualizing single cleavage-ligation events mediated by pfTopI. This result is achieved by a special developed biosensor system in which the catalytic reaction, carried out by pfTopI, is converted to a detectable micrometer-sized product. One interesting findings of this thesis is that there is a considerable difference in the activity response of human and *Plasmodium falciparum* topoisomerase IB regarding the salt tolerance. However, this condition isn't sufficient to carry out a selective detection in biological samples, where the salt concentration is highly variable. The problem has been overcome with the identification of a specific substrate for pfTopI that allows carry out multiplexed single molecule detection in crude and relevant biological samples such as infected blood from sick patients. Since each pfTopI make many catalytic reactions without loosing activity, the sensitivity of the biosensor is expected to compete with the current immunoistochemical based diagnostic tools. Moreover, the tecnique can be applied also on non-invasive samples such as saliva that typically contains only sparse number of *Plasmodium falciparum* parasites.

The sensitivity can be increased by concentrating the RCP signals, which are spread over a large area because the RCA primers are printed by a handheld pipette. The high sensitivity shown by the sepharose beads, detecting the topoisomerases activities, indicates that the concentration of the signals is the right way to proceed. Infact

concentrating RCP signals it's possible to improve sensitivity even further, maybe even at the single cell or single enzyme detection levels. Moreover, the microscopic readout could be replaced with an easy and portable readout device (such as a colorimetric readout) that transforms the biosensor into a more suitable system that could be adeguated to the requirements of the developing countries, that currently suffer the major burden of malaria epidemics.

REFERENCES

Andersen AH., Gocke E., Bonven BJ., Nielsen OF. and Westergaard O. Topoisomerase I has a strong binding preference for a conserved hexadecameric sequence in the promoter region of the rRNA gene from Tetrahymena pyriformis. Nucleic Acids Res. 13(5): 1543-1557 (1985).

Andersen FF., Stougaard M., Jørgensen HL., Bendsen S., Juul S., Hald K., Andersen AH., Koch J. and Knudsen BR. Multiplexed detection of site specific recombinase and DNA topoisomerase activities at the single molecule level. ACS Nano. 3(12): 4043-54 (2009).

Askhin A. Optical trapping and manipulation of neutral particles using lasers. Proc. Natl. Acad. Sci. USA 94: 4853-4860 (1997).

Banér J., M. Nilsson M. Mendel-Hartvig M. and U. Landegren. Signal amplification of padlock probes by rolling circle replication. Nucleic Acids Res. 26 (22): 5073-5078 (1998).

Banér J., NilssonM., Isaksson A, Mendel-Hartvig M., Antson DO. and Landegren U. More keys to padlock probes: mechanisms for high-throughput nucleic acid analysis. Current Opinion in Biotechnology 12(1): 11-15 (2001).

Bannister LH., Hopkins JM., Fowler RE., Krishna S.and Mitchell GH. A brief illustrated guide to the ultrastructure of Plasmodium falciparum asexual blood stages. Parasitology Today 16(10): 427-433 (2000).

Berger JM. and Schoeffler AJ. DNAtopoisomerases : harnessing and constraining energy to govern chromosome topology. Quarterly Reviews of Biophysics 41(1): 41-101 (2008).

Bockelmann U. Single-molecule manipulation of nucleic acids. Curr. Opin. Struct. Biol. 14: 368-373 (2004).

Bonven BJ., Gocke E. and Westergaard O. A High Affinity Topoisomerase I Binding Sequence is Clustered at DNAase I Hypersensitive Sites in Tetrahymena R-Chromatin. Cell. 41: 541-551 (1985).

Bullock P., Champoux JJ. and Botcham M. Association of crossover points with topoisomerase I cleavage sites: a model for nonhomologous recombination. Science 230: 954-958 (1985).

Cavallini M., Facchini M., Albonetti C. and Biscarini F. Single molecule magnets: from thin films to nano-patterns. Phys. Chem. Chem. Phys. 10: 784-793 (2008).

Champoux JJ. Proteins That Affect DNA Conformation. Annu. Rev. Biochem.47: 449-479 (1978).

Champoux JJ. Mechanism of Catalysis by Eukaryotic DNA Topoisomerase I. Adv. Pharmacol. 29A: 71-82 (1994).

Champoux JJ. DNA topoisomerases: structure, function, and mechanism. Annu. Rev. Biochem. 70: 369-413 (2001).

Cheesman SJ. The topoisomerases of protozoan parasites. Parasitology Today. 16(7): 277-281 (2000).

Christiansen K., Svejstrup AB., Andersen AH. and Westergaard O. Eukaryotic Topoisomerase I-Mediated Cleavage Requires Bipartite DNA Interaction. Cleavage of DNA Substrates Containing Strand Interruptions Implicates a Role for Topoisomerase I in Illegitimate Recombination. J. Biol. Chem. 268: 9690-9701 (1993).

Corbett KD. and Berger JM. Structure, molecular mechanisms, and evolutionary relationships in DNA topoisomerases. Annu. Rev. Biophys. Biomol. Struct. 33: 95-118 (2004).

Engel A. and Muller DJ. Observing single biomolecules at work with the atomic force microscope. Nat. Struct.Biol. 7: 715-718 (2000).

Fiorani P., Bruselles A., Falconi M., Chillemi G., Desideri A. and Benedetti P. Single mutation in the linker domain confers protein flexibility and camptothecin resistance to human topoisomerase I. J. Biol. Chem. 278: 43268-43275 (2003).

Fire A. and Xu SQ. Rolling replication of short DNA circles. Proc. Natl. Acad. Sci. U.S.A. 92: 4641-4645 (1995).

Garcia-Carbonero R. and Supko JG. Current perspectives on the clinical experience, pharmacology, and continued development of the camptothecins. Clin Cancer Res 8: 641-661 (2002).

Gilbert W. and Dressler D. DNA replication: the rolling circle model Cold. Spring. Harb. Symp. Quant. Biol. 33: 473-84 (1968).

Gilmour DS. and Elgin SCR. Association of Topoisomerase I with transcriptionally active loci in Drosophila. NCI Monograph 4: 17-21 (1987).

Hammond SM. MicroRNA detection comes of age. Nat. Methods. 3(1): 12-3 (2006).

Hann CL., Carlberg AL. and Bjornsti MA. Intragenic suppressors of mutant DNA Topoisomerase I-induced lethality diminish enzyme binding of DNA. J. Biol. Chem. 273: 31519-31527 (1998).

Hansen SG., Frøhlich RF. and Knudsen BR. Type IB Topoisomerases and Tyrosine Recombinases - Distinct functions within related structural frameworks. Curr. Top. Biochem. Res. 5: 149-159 (2003).

Holden JA. DNA topoisomerases as anticancer drug targets: from the laboratory to the clinic. Curr. Med. Chem. Anticancer Agents.1: 1-25 (2001).

Hsiang YH., Lihou MG. and Liu LF. Arrest of replication forks by drug-stabilized topoisomerase I-DNA cleavable complexes as a mechanism of cell killing by camptothecin. Cancer Res. 49: 5077-5082 (1989).

Jarvius J, Melin J., Goransson J., Stenberg J., Fredriksson S., Gonzalez-Rey C., Bertilsson S. and Nilsson M. Digital quantification using amplified single-molecule detection. Nat. Methods. 3: 725-727 (2006).

Johne R., Müller H., Rector A., van Ranst M. and Stevens H. Rolling-circle amplification of viral DNA genomes using phi29 polymerase. Trends Microbiol. 17(5): 205-211 (2009).

Kasparian J. and Wolf JP. Physics and applications of atmospheric nonlinear optics and filamentation. Opt. Express. 16(1): 466-93 (2008).

Koster DA., Croquette V., Dekker C., Shuman S. and Dekker NH. Friction and torque govern the relaxation of DNA supercoils by eukaryotic topoisomerase IB. Nature 434 (7033): 671-674 (2005).

Koster DA., Crut A., Shuman S., Bjornsti MA and Dekker N. Cellular stretegies for regulating DNA supercoiling: a single molecule perspective. Cell 142: 519-530 (2010).

Krogh BO. and Shuman S. A poxvirus-like type IB topoisomerase family in bacteria. Proc. Natl. Acad. Sci. USA. 99 :1853-1858 (2002).

Kubatkin S., Danilov A., Hjort M., Cornil J., Brédas JL., Stuhr-Hansen N., Hedegård P. and Bjørnholm T. Single-electron transistor of a single organic molecule with access to several redox states. Nature 425(6959): 698-701 (2003).

Leppard JB. and Champoux JJ. Human DNA topoisomerase I: relaxation, roles and damage control. Chromosoma 114: 75-85 (2005).

Leuba SH., Wheeler TB., Cheng CM., LeDuc PR., Fernández-Sierra M. and Quiñones E. Structure and dynamics of single DNA molecules manipulated by magnetic tweezers and or flow. Methods 47(3): 214-22 (2009).

Liu D., Daubendiek SL., Zillman MA., Ryan K. and Kool ET. Rolling circle DNA synthesis: small circular oligonucleotides as efficient templates for DNA polymerases. J. AM. Chem. Soc. 118 (7): 1587-1594 (1996).

Lizardi PM., Huang XH., Zhu ZR., Bray-Ward P., Thomas DC. and Ward DC. Mutation detection and single-molecule counting using

isothermal rolling-circle amplification. Nat. Genet. 19: 225-232 (1998).

Mack A., Sauer B., Abremski K., and Hoess R. Stoichiometry of the Cre Recombinase Bound to the Lox Recombining Site. Nucleic Acids Res. 20: 4451-4455 (1992).

Maul GG., French BT., Van Venrooij WJ and Jiminez SA. Topoisomerase I identified by scleroderma 70 antisera: enrichment of topoisomerase I at the centromere in mouse mitotic cells before anaphase. Proc. Natl. Acad. Sci. USA. 83: 5145-5149 (1986).

McKenzie FE., Sirichaisinthop J., Miller RS., Gasser RA. and Wongsrichanalai C. Dependence of malaria detection and species diagnosis by microscopy on parasite density. Am. J. Trop. Med. Hyg. 69: 372-376 (2003).

Mendis K., Rietveld A., Warsame M., Bosman A., Greenwood B. and Wernsdorfer WH. From malaria control to eradication: the WHO perspective. Tropical Medicine and International Health. 14: 802-809 (2009).

Mikhailenko SV., Oguchi Y. and Ishiwata S. Insights into the mechanisms of myosin and kinesin molecular motors from the single-molecule unbinding force measurements. J. R. Soc. Interface. 7 Suppl 3: 295-306. (2010).

Miller LH., Dror IB., Marsh K. and Doumbo OK. The pathogenic basis of malaria. Nature 415: 673-679 (2002).

Mo YY., Wang P. and Beck WT. Functional Expression of Human DNA Topoisomerase I and its subcellular localization in HeLa cells. Exp. Cell Res. 256: 480-490 (2000).

Moody AH. and Chiodini PL. Non-microscopic method for malaria diagnosis using OptiMAL IT, a second-generation dipstick for malaria pLDH antigen detection. Br. J. Biomed. Sci. 59: 228-231 (2002).

Neuman KC. Single-molecule Measurements of DNA Topology and Topoisomerases. J. Biol. Chem. 285(25): 18967-71 (2010).

Neuman KC. and Block SM. Optical trapping. Rev. Sci. Instrum. 75: 2787-2809 (2004).

Nguyen TH., Lee SM., Na K., Yang S., Kim J. and Yoon ES. An improved measurement of dsDNA elasticity using AFM. Nanotechnology. 21(7): 75101. (Epub 2010 Jan 21).

Nilsson M., Krejci K., Koch J., Kwiatkowski M., Gustavsson P. and Landegren U. Padlock probes reveal single-nucleotide differences, parent of origin and in situ distribution of centromeric sequences in human chromosomes 13 and 21. Nat. Genet. 16: 252-255 (1997).

Nilsson M., Malmgren H., Samiotaki M., Kwiatkowski M., Chowdhary B.P. and Landegren U. Padlock probes: Circularizing oligonucleotides for localized DNA detection. Science 265: 2085-2088 (1994).

Patel A., Shuman S. and Mondragon A. Crystal structure of a bacterial type IB DNA topoisomerase reveals a preassembled active site in the absence of DNA. J. Biol. Chem. 281: 6030-6037 (2006).

Perkins MD. and Bell DR. Working without a blindfold: the critical role of diagnostics in malaria control. Malar. J. 7(1): S5 (2008).

Pommier Y. DNA topoisomerase I inhibitors: chemistry, biology, and interfacial inhibition. Chem. Rev. 109: 2894-2902 (2009).

Pommier Y., Leo E., Zhang HL and Marchand C. DNA Topoisomerases and their poisoning by anticancer and antibacterial drugs. Chem. Biol. 17(5): 421-433 (2010).

Pope LH., Bennink ML. and Greve J. Optical tweezers stretching of chromatin. J. Muscle Res. Cell Motil. 23(5-6): 397-407 (2002).

Qian XH., Inman RB. and Cox MM. Reactions between Half- and Full-FLP Recombination Target Sites. A Model System for Analyzing Early Steps in FLP Protein-Mediated Site-Specific Recombination. J. Biol. Chem. 267: 7794-7805 (1992).

Rasheed ZA and Rubin EH. Mechanisms of resistance to topoisomerase I-targeting drugs. Oncogene 22: 7296-7304 (2003).

Redinbo MR., Stewart L., Kuhn P., Champoux JJ. and Hol WG. Crystal structures of human topoisomerase I in covalent and noncovalent complexes with DNA. Science 279: 1504-1513 (1998).

Reguera RM., Redondo CM., Gutierrez de Prado R., Pérez-Pertejo Y. and Balaña-Fouce R. DNA topoisomerase I from parasitic protozoa: a potential target for chemotherapy. Biochim. Biophys. Acta. 1759: 117-131 (2006).

Riou JF., Gabillot M., Philippe M., Schrevel J. and Riou G. Purification and characterization of Plasmodium berghei DNA topoisomerases I and II: drug action, inhibition of decatenation and relaxation, and stimulation of DNA cleavage. Biochemistry. 25(7): 1471-1479 (1986).

Sako Y. and Yanagida T. Single-molecule visualization in cell biology. Nat Rev Mol Cell Biol. Suppl:SS1-5 (2003).

Schopf E., Fischer NO., Chen Y., and Tok JB. Sensitive and selective viral DNA detection assay via microbead-based rolling circle amplification. Bioorg Med Chem Lett. 18(22): 5871-4 (2008).

Schopf E. and Chen Y. Attomole DNA detection assay via rolling circle amplification and single molecule detection. Analytical Biochemistry. 397: 115-117 (2010).

Seidel R and Dekker C. Single-molecule studies of nucleic acid motors. Current Opinion in Structural Biology. 17: 80-86 (2007).

Shaevitz JW., Abbondanzieri EA., Landick R. and Block SM.: Backtracking by single RNA polymerase molecules observed at near-base-pair resolution. Nature 426: 684-687 (2003).

Sharma A., Hanai R. and Mondragon A. Crystal structure of the aminoterminal fragment of vaccinia virus DNA topoisomerase I at 1.6 A resolution. Structure 2 : 767-777 (2004).

Shchepinov MS., Udalova IA., Bridgman AJ. And Southern EM. Oligonucleotide dendrimers: synthesis and use as polylabelled DNA probes. Nucleic Acids Res. 25: 4447-4454 (1997).

Slesarev AI., Stetter KO., Lake JA., Gellert M., Krah R. and Kozyavkin SA. DNA topoisomerase V is a relative of eukaryotic topoisomerase I from a hyperthermophilic prokaryote. Nature 364: 735-737 (1993).

Spencer HC., Collins WE., Chin W. and Skinner JC. The enzyme-linked immunosorbent assay (ELISA) for malaria. I. The use of in

vitro-cultured Plasmodium falciparum as antigen. Am. J. Trop. Med. Hyg. 28: 927-932 (1979).

Stewart L., Ireton GC. and Champoux JJ. Reconstitution of human topoisomerase I by fragment complementation. J. Biol. Mol. 269: 355-372 (1997).

Stewart L., Redinbo MR., Qiu X., Hol WGL. and Champoux JJ. A model for the mechanism of human topoisomerase I. Science 279: 1534-1540 (1998).

Stougaard M., Lohmann JS., Mancino A., Celik S., Andersen FF., Koch J. and Knudsen BR. Single-molecule detection of human topoisomerase I cleavage-ligation activity. ACS Nano 27, 3(1): 223-33 (2009).

Stougaard M., Lohmann JS., Zajac M., Hamilton-Dutoit S. and Koch J. In situ detection of non-polyadenylated RNA molecules using Turtle Probes and target primed rolling circle PRINS. BMC Biotechnol. 7, 69 (2007).

Strick TR., Croquette V. and Bensimon D. Single-molecule analysis of DNA uncoiling by a type II topoisomerase. Nature 404 (6780): 901-904 (2000).

Sturm A., Amino R., Van de Sand C., Regen T., Retzlaff S., Rennenberg A., Krueger A., Pollok JM., Menard R. and Heussler VT.

Manipulation of host hepatocytes by the malaria parasite for delivery into liver sinusoids. Science 313 (5791): 1287-1490 (2006).

Subramani R., Juul S., Rotaru A., Andersen FF., Gothelf KV., Mamdouh W., Besenbacher F., Dong W. and Knudsen BR. A novel secondary DNA binding site in human Topoisomerase I unravelled by using a 2D DNA origami platform. ACS Nano (Epub a print) 2010.

Sulzer AJ., Wilson M. and Hall EC. Indirect fluorescentantibody tests for parasitic diseases. V. An evaluation of a thick-smear antigen in the IFA test for malaria antibodies. Am. J. Trop. Med. Hyg. 18: 199-205 (1969).

Tanizawa A., Kohn KW. and Pommier Y. Induction of cleavage in topoisomerase I c-DNA by topoisomerase I enzymes from calf thymus and wheat germ in the presence and absence of camptothecin. Nucleic Acids Res. 21: 5157-66 (1993).

Tesauro C., Fiorani P., D'Annessa I., Chillemi G., Turchi G. and Desideri A. Erybraedin C, a natural compound from the plant Bituminaria bituminosa, inhibits both the cleavage and religation activities of human topoisomerase I. Biochem. J. 425(3): 531-9 (2010).

Tosh K., Cheesman S., Horrocks P. and Kilbey B. Plasmodium falciparum: stage-related expression of topoisomerase I. Exp. Parasitol. 91(2): 126-132 (1999).

Tosh K. and Kilbey B. The gene encoding topoisomerase I from the human malaria parasite Plasmodium falciparum. Gene. 163(1): 151-154 (1995).

van Mameren J., Peterman EJ. and Wuite GJ. See Me, Feel Me: Methods to Concurrently Visualize and Manipulate Single DNA Molecules and Associated Proteins. Nucleic Acids Res. 36: 4381-4389 (2008).

Voigt NV., Tørring T., Rotaru A., Jacobsen MF., Ravnsbaek JB., Subramani R., Mamdouh W., Kjems J., Mokhir A., Besenbacher F. and Gothelf KV. Single-molecule chemical reactions on DNA origami. Nat. Nanotechnol. 5(3): 200- 203 (2010).

Vologodskii AV. and Cozzarelli NR. Conformational and thermodynamic properties of supercoiled DNA. Annu. Rev. Biophys. Biomol. Struct. 23: 609-643 (1994).

Walker GT., Fraiser MS., Schram JL., Little MC., Nadeau JG. and Malinowski DP. Strand displacement amplification—an isothermal, in vitro DNA amplification technique. Nucleic Acids Res. 20: 1691-1696 (1992).

Walker GT., Little MC., Nadeau JG. and Shank DD. Isothermal in vitro amplification of DNA by a restriction enzyme/DNA polymerase system. Proc. Natl. Acad. Sci. U. S. A. 89(1): 392-396 (1992).

Wang JC. Interaction between DNA and Escherichia coli protein omega. J. Mol. Biol. 55: 523-533 (1971).

Wang JC. DNA topoisomerases. Annu. Rev. Biochem. 65: 635-692 (1996).

Wang JC. Cellular roles of DNA topoisomerases: a molecular perspective. Nat. Rev. Mol. Cell Biol. 3: 430-440 (2002).

Wang K., Forbes JG. and Jin AJ. Single molecule measurements of titin elasticity. Prog. Biophys. Mol. Biol. 77(1): 1-44 (2001).

Winn-Deen ES. Automation of molecular genetic methods-part 2: DNA amplification techniques. J. Clin. Ligand Assay. 19: 21-26 (1996).

Wongsrichanalai C., Barcus MJ., Muth S., Sutamihardja A. and Wernsdorfer WH. A review of malaria diagnostic tools: microscopy and rapid diagnostic test (RDT). Am J Trop Med Hyg. 77(6): 119-127 (2007).

World Malaria Report, World Health Organisation, Geneva, 2009.

Wu J. and Liu LF. Processing of topoisomerase I cleavable complexes into DNA damage by transcription. Nucleic Acids Research 25(21): 4181-4186 (1997).

Yang L., Wold MS., Li JJ., Kelly TJ. and Liu LF. Roles of DNA topoisomerases in simian virus 40 DNA replication in vitro. Proc. Natl. Acad. Sci. USA. 84: 950-954 (1987).

Yao NY., Georgescu RE., Finkelstein J. and O'Donnell ME. Single-molecule analysis reveals that the lagging strand increases replisome processivity but slows replication fork progression. Proc Natl Acad Sci USA. 106(32): 13236-13241 (2009).

Zhang H., Meng LH., Zimonjic, DB., Popescu NC. and Pommier Y. Thirteen- exon-motif signature for vertebrate nuclear and mitochondrial type IB topoisomerases. Nucleic Acids Res. 32: 2087-2092 (2004).

ABBREVIATIONS

AA: Amino acids

Amol: Attomole

AMS: Ammonium Sulfate

Bp: Base pair

BSA: Bovine Serum Albumin

DI/DC: Polydeoxyinosinic-Deoxycytidylic Acid

DTT: Dithiothreitol

EDTA: Ethylenediaminetetraacetic acid

ELISA: Enzyme-Linked Immunosorbent Assay

ELU: Eluition buffer

EtBr: Ethidium Bromide

FISH: Fluorescent In Situ Hybridization

KDa: Kilo Dalton

LiAc: Lithium Acetate

NP40: Nonyl phenoxypolyethoxylethanol.

PBS: Phosphate Buffer Saline

PMSF: Phenylmethyl Sulfonyl Fluoride, protease inhibitor.

RPM: Rotation Per Minute

SDS: Sodium Dodecyl Sulfate

SNP: Single Nucleotide Polymorphism

TBE: Tris-Borate-EDTA

TopI: Topoisomerase I

CURRICULUM VITAE

Education

2008-Present Ph.D. student in Nanostructures and Nanotechnologies, University of Rome Tor Vergata and University of Milan Bicocca, Italy.

2007 Degree in Molecular Biology "110/110 cum laude" Department of Biology, University of Rome Tor Vergata, Italy.

Research experience

16/08/2010-31/10/2010: Exchange PhD student in the laboratory of Prof. B.R.Knudsen, Department of Molecular Biology, University of Aarhus, Denmark.

17/08/2009-28/02/2010: Exchange PhD student in the laboratory of Prof. B.R.Knudsen, Department of Molecular Biology, University of Aarhus, Denmark.

2008-present: Graduate PhD student in the laboratory of Prof. Alessandro Desideri, Department of Biology, University of Rome Tor Vergata, Italy.

2005-2007: Undergraduate fellow in the laboratory of Prof. Alessandro Desideri, Department of Biology, University of Rome Tor Vergata, Italy.

Experties

PCR, site direct mutagenesis, bacterial and yeast growth and trasformation, preparation of plasmidic DNA, cloning, gel electrophoresis, DNA restriction digestion, protein purification, chromatography, SDS page, western blotting, enzymatic assays, TCA preparation, cellular colture, mammalian cellular grow inhibition assays, nuclear extracts extraction, assays with radiolabeled oligos, EMSA, single molecule detection of DNA Topoisomerase's activity, fluorescence microscopy, q-nano device (I-zone), RCA based assay with sepharose beads.

Publications

1) Tordrup D., **Tesauro C**., Fiorani P., Nielsen C., Gentry A., Osheroff N., Desideri A., Knudsen BR. and Andersen F. "Cloning, Purification, and Characterization of Plasmodium falciparum Topoisomerase I: Catalytic Activity and Interaction with Camptothecin". Submitted to Biochemistry (10/12/2010).

2) **Tesauro C**., Fiorani P., D'Annessa I., Chillemi G., Turchi G. and Desideri A. "Erybraedin C, a natural compound from the plant

Bituminaria bituminosa, inhibits both the cleavage and religation activities of human topoisomerase I". Biochemical Journal. 425(3): 531-9 (2010).

3) **Tesauro C.,** Stougaard M., Tordrup D., Fiorani P., Petersen JE., Desideri A., Koch J., Knudsen BR and Andersen FF. "Development of a novel *Plasmodium falciparum* Topoisomerase I specific biosensor for diagnosis of Malaria". Expected to be submitted to Nature Nanotechnology.

4) Morozzo della Rocca B., Smith CI., **Tesauro C**., Desideri A. and Weightman P. "Adsorption of the cysteine-tryptophan dipeptide at the Au(110)/liquid interface studied using reflection anisotropy spectroscopy" Surface Science 604: 2170-2176 (2010).

5) Fiorani P. - **Tesauro C**., Mancini G., Chillemi G., D'Annessa I., Graziani G., Tentori L., Muzi A. and Desideri A. "Evidence of the crucial role of the linker domain on the catalytic activity of human topoisomerase I by experimental and simulative characterization of the Lys681Ala mutant." Nucleic acid research. 37(20): 6849-58 (2009).

6) Castelli S., Campagna A., Vassallo O., **Tesauro C**., Fiorani P., Tagliatesta P., Oteri F., Falconi M., Majumder HK. and Desideri A. "Conjugated eicosapentaenoic acid inhibits human topoisomerase IB with a mechanism different from camptothecin". Arch. Biochem. Biophys. 486(2): 103-10 (2009).

7) Chillemi G., Fiorani P., Bruselles A., Castelli S., Campagna A., Sarra O., **Tesauro C**., Fiorentini M., Vassallo O., D'Annessa I., Santoleri S. and Desideri A. "Role of flexibility and long range communication on the function of human topoisomerase I". Ital. J. Biochem. 56(2): 110-4 (2007).

Congresses

- 8th INANO Annual meeting. Aarhus, Denmark 20/01/2010.
- Nanotech 2009, 28-30 September 2009, Berlin.
- 51° National SIB Congress, Riccione, Italy. September 2006.

Poster

- Andersen F., Stougaard M., **Tesauro C**., Tordrup D., Juul S., Bendsen S., Nielsen C., Orecchioni S., Andersen AH., Koch J. and Knudsen BR. “Detection of DNA Topoisomerase I and related enzyme activities at the single molecule level”.

- Fiorani P., Castelli S., Sarra O., **Tesauro C**. and Alessandro Desideri. “The camptothecin-resistant human topoisomerase I Glu418Lys mutant shows a different DNA sequence specificity”.

TALK

4/12/2009: Department of Molecular Biology meeting, University of Aarhus “Novel assays and read out formats for the activity´s detection of DNA interacting and modifyng enzyme at single molecule level”.

ACKNOWLEDGMENTS

This work was done under supervision of Professor Alessandro Desideri, from University of Roma Tor Vergata and Professor Birgitta Knudsen, from University of Århus, Denmark. I am grateful for their support, insightful advice, scientific guidance and inspiring discussions.

I would like to thank Paola Fiorani for being my mentor since my undergraduate research period, Magnus Stougaard and Simon Bendsen for their help and numerous suggestions on how to manage with microscope and Félicie F. Andersen for her helpful contribution on thesis review. Gratitude is also expressed to David Tordrup, Sissel Juul and Gerda Hübner, that not only provided the purified proteins but were also friendly and supportive during my visiting period at Århus University.

I must also acknowledge all my Rome lab friends: Blasco, Alice, Oscar, Ilda, Barbara and Laura to whom it would take too long to list all the reasons. I can't forget to thank Eric Schopf for his kindness answering all my questions by e-mail. Finally, special thanks goes to my loved Andrea for the support he provided me through these years and because, without whose love, encouragement and editing assistance, I would not have completed this thesis.